Carbon−Nitrogen-Bond-Forming Reductive Elimination of Arylamines from Palladium(II) Phosphine Complexes

Michael S. Driver and John F. Hartwig*

Contribution from the Department of Chemistry, Yale University, P.O. Box 208107 New Haven, Connecticut 06520-8107

Received April 3, 1997[⊗]

Abstract: A series of monomeric palladium amido complexes of the form *trans*-$(PPh_3)_2Pd(Ar)(NAr'_2)$ and (DPPF)-$Pd(Ar)(NAr'_2)$ (DPPF = 1,1′-bis(diphenylphosphino)ferrocene) and dimeric palladium amido complexes of the form $\{(PPh_3)Pd(Ar)(\mu\text{-}NHR)\}_2$ (R = Ph, *t*-Bu) have been prepared by the reaction of lithium and potassium amides with palladium aryl halide complexes. An X-ray crystal structure of (DPPF)Pd(*p*-$NMe_2C_6H_4$)[N(*p*-$CH_3C_6H_4)_2$] was obtained. Upon thermolysis in the presence of PPh_3, serving as a trapping agent, both the monomeric and dimeric palladium amido complexes underwent C−N-bond-forming reductive elimination to form arylamines in high yields along with a Pd(0) species. Reductive elimination was also observed from azametallacycle $(PPh_3)Pd(\eta^2\text{-}C_6H_4C_6H_4\text{-}NH)$, to form carbazole and $Pd(PPh_3)_4$ at room temperature. Mechanistic studies on the reductive elimination reactions of the monomeric PPh_3-ligated amido complexes indicated the presence of two competing pathways for the formation of amine. At low [PPh_3], reductive elimination occurs via phosphine dissociation to form a three-coordinate intermediate; however, as [PPh_3] is increased, a pathway of reductive elimination from a four-coordinate complex becomes dominant. The DPPF-ligated palladium amido complexes directly eliminated amine from the four-coordinate complex. The mechanism of the reductive elimination from dimeric palladium amido complexes was also studied. These complexes undergo reductive elimination of amine via dimer dissociation to generate a three-coordinate intermediate analogous to those formed by the PPh_3-ligated monomeric amido complexes. The C−N-bond forming reductive elimination reactions were accelerated by electron-withdrawing groups on the Pd bound aryl group and by electron-donating groups on the amido ligand, suggesting that the aryl group acts as an electrophile and the amido ligand acts as a nucleophile.

Introduction

Low-valent late-transition-metal amido complexes are highly reactive molecules involved in catalysis, but for which little fundamental reactivity is known. These complexes are believed to be reactive because of a mismatch between the soft transition-metal center with the hard amido ligand.[1,2] Metal−amido complexes have been proposed as intermediates in a number of catalytic processes. The catalytic hydrogenation of imines[3−21] and nitriles[22,23] is thought to proceed via metal−amido intermediates. More recently, a catalytic process which leads to the addition of aniline across an olefin has been reported to form a metal−amido intermediate through oxidative addition of aniline to an iridium center.[24] Metal−amido complexes have also been implicated as key intermediates present in the palladium-catalyzed amination of aryl halides and aryl triflates.[25−34] Yet, synthetic routes to the reactive intermediates proposed in these

[⊗] Abstract published in *Advance ACS Abstracts,* August 15, 1997.

(1) Pearson, R. G. *J. Am. Chem. Soc.* **1963**, *85*, 3533.
(2) Pearson, R. G. *J. Chem. Educ.* **1968**, *45*, 643.
(3) Amrani, Y.; Lecomte, L.; Simou, D.; Bakos, J.; Toth, I.; Heil, B. *Organometallics* **1989**, *8*, 542.
(4) Bakos, J.; Toty, I.; Heil, B.; Marko, L. *J. Organomet. Chem.* **1985**, *279*, 23.
(5) Bakos, J.; Toth, I.; Heil, B.; Szalontai, G.; Parkanyi, L.; Fulop, V. *J. Organomet. Chem.* **1989**, *370*, 263.
(6) Bakos, J.; Orosz, A.; Heil, B.; Laghmari, M.; Lhoste, P.; Sinou, D. *J. Chem. Soc., Chem. Commun.* **1991**, 1684.
(7) Becalski, A. G.; Cullen, W. R.; Fryzuk, M. D.; James, B. R.; Kang, G. J.; Rettig, S. J. *Inorg. Chem.* **1991**, *30*, 5002−5008.
(8) Burk, M. J.; Feaster, J. E. *J. Am. Chem. Soc.* **1992**, *114*, 6266.
(9) Chan, Y. N. C.; Osborn, J. A. *J. Am. Chem. Soc.* **1990**, *112*, 9400.
(10) Cullen, W. R.; Fryzuk, M. D.; James, B. R.; Kutney, J. P.; Kang, G. J.; Herb, G.; Thorburn, I. S.; Spogliarich, R. *J. Mol. Catal.* **1990**, *62*, 243.
(11) Imine hydrogenation catalyzed by rhodium and iridium complexes would be expected to occur through an amide complex. However, mechanistic data is scarce. A direct observation of imine insertion that produces an amide complex potentially similar to those in catalytic systems is the following: Fryzuk, M. D.; Piers, W. E. *Organometallics* **1990**, *9*, 986−98.
(12) For a recent review see: James, B. R. *Chem. Ind.* **1995**, *62*, 167−180.
(13) Kang, G. J.; Cullen, W. R.; Fryzuk, M. D.; James, B. R.; Kutney, J. P. *J. Chem. Soc., Chem. Commun.* **1988**, 1466.
(14) Longley, C. J.; Goodwin, T. J.; Wilkinson, G. *Polyhedron* **1986**, *5*, 1625.
(15) Ng, Y.; Chan, C.; Meyer, D.; Osborm, J. A. *J. Chem. Soc., Chem. Commun.* **1990**, 869.
(16) Spindler, F.; Pugin, B.; Blaser, H. U. *Angew. Chem., Int. Ed. Engl.* **1990**, *29*, 558.
(17) Vastag, S.; Bakos, J.; Toros, S.; Takach, N. E.; King, R. B.; Heil, B.; Marko, L. *J. Mol. Catal.* **1984**, *22*, 283.
(18) Willoughby, C. A.; Buchwald, S. L. *J. Am. Chem. Soc.* **1992**, *114*, 7562.
(19) Willoughby, C. A.; Buchwald, S. L. *J. Org. Chem.* **1993**, *58*, 7627.
(20) Willoughby, C. A.; Buchwald, S. L. *J. Am. Chem. Soc.* **1994**, *116*, 11703−11714.
(21) Willoughby, C. A.; Buchwald, S. L. *J. Am. Chem. Soc.* **1994**, *116*, 8952.
(22) Armor, J. N. *Inorg. Chem.* **1978**, *17*, 203−213.
(23) Yoshida, T.; Okano, T.; Otsuka, S. *J. Chem. Soc., Chem. Commun.* **1979**, 870.
(24) Casalnuovo, A. L.; Calabrese, J. C.; Milstein, D. *J. Am. Chem. Soc.* **1988**, *110*, 6738−6744.
(25) Kosugi, M.; Kameyama, M.; Migita, T. *Chem. Lett.* **1983**, 927−928.
(26) Kosugi, M.; Kameyama, M.; Sano, H.; Migita, T. *Nippon Kagaku Kaishi* **1985**, *3*, 547−551.
(27) Paul, F.; Patt, J.; Hartwig, J. F. *J. Am. Chem. Soc.* **1994**, *116*, 5969−5970.
(28) Guram, A. S.; Buchwald, S. L. *J. Am. Chem. Soc.* **1994**, *116*, 7901−7902.
(29) Louie, J.; Paul, F.; Hartwig, J. F. *Organometallics* **1996**, *15*, 2794−2805.
(30) Louie, J.; Hartwig, J. F. *Tetrahedron Lett.* **1995**, *36*, 3609.
(31) Guram, A. S.; Rennels, R. A.; Buchwald, S. L. *Angew. Chem., Int. Ed. Engl.* **1995**, *34*, 1348.
(32) Driver, M. S.; Hartwig, J. F. *J. Am. Chem. Soc.* **1996**, *118*, 7217−7218.

S0002-7863(97)01057-3 CCC: $14.00

catalytic processes are not well developed and have attracted significant attention only recently. The high reactivity of metal−amido complexes as well as their facile decomposition through low-energy pathways such as β-hydrogen elimination[35,36] has limited the number of isolated amido complexes. As a consequence, the fundamental reaction chemistry of metal−amido complexes has remained undeveloped.

Presently, metal complexes containing arylamido,[35−47] silylamido,[35,36,48] and parent amido[35,36,49−51] ($-NH_2$) ligands have been characterized. Alkylamido complexes have remained rare.[46,52−56] Arylamido compounds have displayed insertion chemistry,[35−47] exchanges with even mildly acidic H−X bonds,[35−47,57] and in some cases N−H-bond-forming reactions.[35,36,43,45,46,58] Yet, amido complexes which undergo reductive elimination to form the carbon−nitrogen bond of amines have been observed in only a few cases.[54,59−61] Although reductive eliminations to form C−C and C−H bonds are among the fundamental reactions of organometallic chemistry, little is known about analogous reactions forming C−N bonds. A better understanding of C−N-bond-forming reductive elimination reactions is essential for the further development of catalytic processes that construct amines and nitrogen heterocycles. Previously, we have communicated our preliminary mechanistic results on C−N-bond-forming reductive elimination from some isolated palladium(II) amido complexes.[54] We now report the results of an extensive synthetic and mechanistic study of C−N-bond-forming reductive eliminations from a series of monomeric and dimeric palladium(II) amido complexes.

Scheme 1

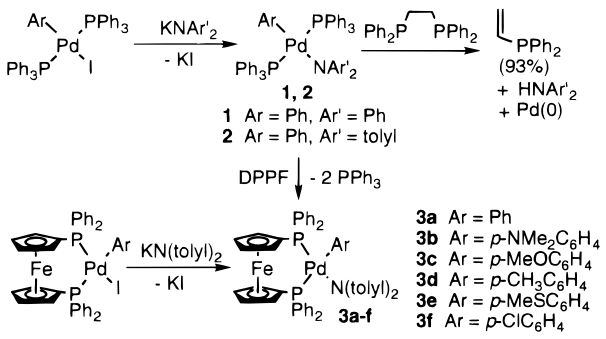

Monomeric palladium complexes of the form $L_2PdAr(NAr'_2)$ have been prepared, and they reductively eliminate arylamine, $ArNAr'_2$. The reductive elimination chemistry of these complexes involves two concurrent pathways, and it is the existence of these two pathways that allows for aryl halide amination reactions to occur with complexes containing chelating ligands. Monomeric complexes containing chelating phosphine ligands and a variety of aryl groups and amido groups have revealed the electronic properties of the transition state for C−N-bond-forming reductive elimination. We have also prepared some dimeric palladium(II) amido complexes, one of which is a rare example of an alkylamido complex. The dimeric amido complexes also reductively eliminate arylamine. In this case, kinetic studies show that the bridging interaction is cleaved either reversibly or irreversibly depending on the amido group and that the resulting three-coordinate intermediate undergoes elimination of amine.

Results

A. Synthesis and Characterization of Palladium(II) Amido Complexes. 1. Monomeric Palladium Amido Complexes. The syntheses of *trans*-$(PPh_3)_2Pd(C_6H_5)[N(C_6H_5)_2]$ (**1**) and *trans*-$(PPh_3)_2Pd(C_6H_5)[N(p\text{-}CH_3C_6H_4)_2]$ (**2**) are summarized in Scheme 1. Addition of $KN(C_6H_5)_2$ or $KN(C_6H_4p\text{-}Me)_2$ to a THF solution of *trans*-$(PPh_3)_2Pd(C_6H_5)(I)$ led to the clean formations of **1** or **2**, which were isolated in 86% and 78% yields, respectively, after crystallization from THF/Et_2O. Complexes **1** and **2** were characterized by standard spectroscopic and microanalytical techniques. The formation of complexes **1** and **2** was signified by a shift of the $^{31}P\{^1H\}$ NMR resonance (**1** δ 21.4, s; and **2** δ 21.0, s) upfield from that of the starting palladium aryl halide complex (δ 24.3, s), the observation of tolyl methyl groups for **2**, and the appropriate aryl $^{13}C\{^1H\}$ signals. Both complexes **1** and **2** are red, and the UV−vis spectrum of **1** showed an absorbance at $\lambda_{max} = 489.6$ nm with an extinction coefficient of $\epsilon = 800\ cm^{-1}\ M^{-1}$.

2. Monomeric Palladium Amido Complexes Containing *Cis*-Chelating Phosphines. The observation that reductive elimination of arylamine can occur from a four-coordinate palladium amido complex (*vide infra*) led us to seek the synthesis of palladium amido complexes possessing *cis*-chelating phosphine ligands. Such *cis*-chelated complexes would allow us to observe directly the C−N-bond-forming reductive elimination in the absence of competing processes such as phosphine dissociation and *cis/trans* isomerization. Despite kinetic results described below that demonstrate elimination can occur from four-coordinate complexes, the general chemistry of palladium amido aryl complexes with chelating phosphine ligands was dominated by reactions other than C−N-bond-forming reductive

(33) Wolfe, J. P.; Wagaw, S.; Buchwald, S. L. *J. Am. Chem. Soc.* **1996**, *118*, 7215−7216.
(34) Louie, J.; Driver, M. S.; Hamann, B. C.; Hartwig, J. F. *J. Org. Chem.* **1997**, in press.
(35) Bryndza, H. E.; Tam, W. *Chem. Rev.* **1988**, *88*, 1163 and references therein.
(36) Fryzuk, M. D.; Montgomery, C. D. *Coord. Chem. Rev.* **1989**, *95*, 1−40 and references therein.
(37) Glueck, D. S.; Winslow, L. J.; Bergman, R. G. *Organometallics* **1991**, *10*, 1462−1479.
(38) Glueck, D. S.; Bergman, R. G. *Organometallics* **1991**, *10*, 1479−1486.
(39) Hartwig, J. F.; Andersen, R. A.; Bergman, R. G. *J. Am. Chem. Soc.* **1989**, *111*, 2717.
(40) Hartwig, J. F.; Bergman, R. G.; Andersen, R. A. *J. Am. Chem. Soc.* **1991**, *113*, 6499.
(41) Hartwig, J. F.; Andersen, R. A.; Bergman, R. G. *Organometallics* **1991**, *10*, 1875.
(42) Martin, G. C.; Boncella, J. M.; Wurcherer, E. J. *Organometallics* **1991**, *10*, 2804.
(43) Seligson, A. L.; Cowan, R. L.; Trogler, W. C. *Inorg. Chem.* **1991**, *30*, 3371.
(44) For a well-characterized example and related references, see: Ruiz, J.; Martinez, M. T.; Vicente, C.; Garcia, G.; Lopez, G.; Chaloner, P.; Hitchcock, P. B. *Organometallics* **1993**, *12*, 4321.
(45) Rahim, M.; White, C.; Rheingold, A. L.; Ahmed, K. J. *Organometallics* **1993**, *12*, 2401−2403.
(46) Rahim, M.; Bushweller, C. H.; Ahmed, K. J. *Organometallics* **1994**, *13*, 4952−4958.
(47) Boncella, J. M.; Villanueva, L. A. *J. Organomet. Chem.* **1994**, *465*, 297−304.
(48) Fryzuk, M. D.; Montgomery, C. D.; Rettig, S. J. *Organometallics* **1991**, *10*, 467−473.
(49) Joslin, F. L.; Johnson, M. P.; Mague, J. T.; Roundhill, D. M. *Organometallics* **1991**, *10*, 2781.
(50) Park, S.; Rheingold, A. L.; Roundhill, D. M. *Organometallics* **1991**, *10*,
(51) Koelliker, R.; Milstein, D. *J. Am. Chem. Soc.* **1991**, *113*, 8524.
(52) Klein, D. P.; Hayes, J. C.; Bergman, R. G. *J. Am. Chem. Soc.* **1988**, *110*, 3704.
(53) Dewey, M. A.; Knight, A.; Arif, A.; Gladysz, J. A. *Chem. Ber.* **1992**, *125*, 815−824.
(54) Driver, M. S.; Hartwig, J. F. *J. Am. Chem. Soc.* **1995**, *117*, 4708−4709.
(55) Driver, M. S.; Hartwig, J. F. *J. Am. Chem. Soc.* **1996**, *118*, 4206−4207.
(56) Hartwig, J. F. *J. Am. Chem. Soc.* **1996**, *118*, 7010.
(57) Bryndza, H. E.; Fong, L. K.; Paciello, R. A.; Tam, W.; Bercaw, J. E. *J. Am. Chem. Soc.* **1987**, *109*, 1444.
(58) Rahim, M.; Ahmed, K. J. *Organometallics* **1994**, *13*, 1751−1756.
(59) Villanueva, L. A.; Abboud, K. A.; Boncella, J. M. *Organometallics* **1994**, *13*, 3921−3931.
(60) Koo, K.; Hillhouse, G. L. *Organometallics* **1995**, *14*, 4421−4423.
(61) Matsunaga, P. T.; Hess, C. R.; Hillhouse, G. L. *J. Am. Chem. Soc.* **1994**, *116*, 3665−3666.

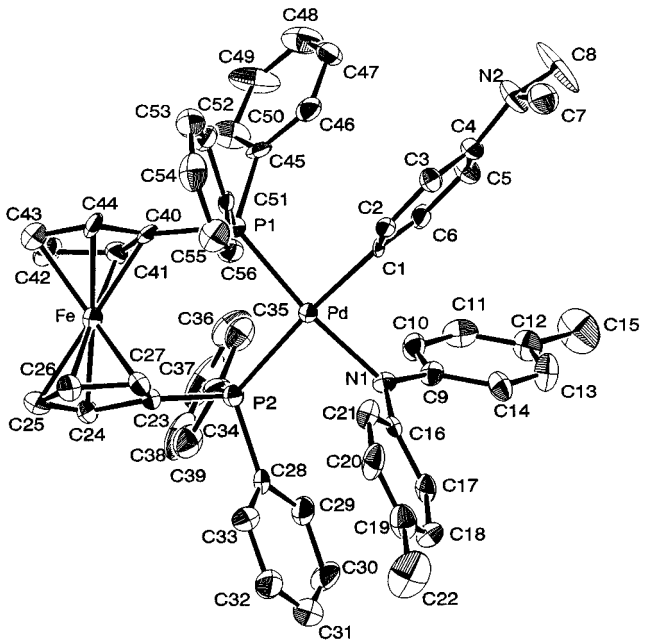

Figure 1. ORTEP Drawing of (DPPF)Pd[*p*-N(CH$_3$)$_2$C$_6$H$_4$][N(*p*-CH$_3$C$_6$H$_4$)$_2$] (**3b**). Hydrogen atoms are omitted for clarity.

elimination. The addition of DPPE (1,2-bis(diphenylphosphino)ethane) to a solution of **2** led to the decomposition of the DPPE backbone by P−C bond cleavage and formation of vinyldiphenylphosphine[62] in 93% yield, as shown in Scheme 1. Addition of other chelating phosphine ligands such as DPPP (1,3-bis(diphenylphosphino)propane), DPPBz (1,2-bis(diphenylphosphino)benzene), and DPPEn (1,2-bis(diphenylphosphino)-ethylene) did not produce stable amido complexes, and no triarylamine products were observed.

Nevertheless, we found that amido complexes containing the chelating phosphine ligand DPPF (DPPF = 1,1′-bis(diphenylphosphino)ferrocene) could be isolated or observed spectroscopically and that these complexes produced arylamines in high yields by reductive elimination. As shown in Scheme 1, addition of DPPF to a THF solution of **2** generated the DPPF-ligated product **3a** in 54% yield. A series of monomeric palladium ditolylamido complexes **3a**−**f** possessing the *cis*-chelating ligand DPPF were prepared by addition of KN(*p*-CH$_3$C$_6$H$_4$)$_2$ to (DPPF)Pd(Ar)(X) complexes (Ar = *p*-NMe$_2$C$_6$H$_4$, *p*-CH$_3$OC$_6$H$_4$, *p*-CH$_3$C$_6$H$_4$, *p*-CH$_3$SC$_6$H$_4$, *p*-ClC$_6$H$_4$)[63] as shown in Scheme 1 and were isolated in yields between 62% and 78% by recrystallization from THF/Et$_2$O. These complexes displayed two sharp doublets in the ^{31}P{^{1}H} NMR spectrum, demonstrating the cis, four-coordinate geometry shown in Scheme 1.

3. X-ray Crystal Structure of Complex 3b. During our studies on the DPPF-ligated palladium amido complexes, we were able to obtain X-ray quality crystals of complex **3b**. The ORTEP drawing of **3b** is shown in Figure 1; data collection and refinement parameters, bond distances, and bond angles are provided in Tables 1−3. Complex **3b** crystallized in the triclinic space group P_{-1} (no. 2). The geometry at the Pd is square-planar; the sum of the four angles at palladium is 359.97°. The P−Pd−P bite angle is believed to be important in controlling the rates for reductive elimination. The 100.47° angle in **3b** is larger than other neutral palladium DPPF complexes.[64−67] The

Table 1. Data Collection and Refinement Parameters for X-ray Structure of (DPPF)Pd[*p*-N(CH$_3$)$_2$C$_6$H$_4$][N(*p*-CH$_3$C$_6$H$_4$)$_2$]

empirical formula	C$_{56}$H$_{52}$N$_2$P$_2$FePd·C$_3$H$_6$O$_{0.75}$
formula weight	1031.31
crystal color/habit	red plates
crystal system	triclinic
lattice parameters:	
	a = 11.086(4) Å
	b = 14.901(3) Å
	c = 16.329(3) Å
	α = 73.41(2) °
	β = 78.92(2) °
	γ = 89.16(2) °
volume	2534(2)
space group	P_{-1} (no. 2)
Z value	2
diffractometer	Enraf-Nonius CAD-4
radiation	Mo Kα (λ = 0.710 69 Å)
T	−60 °C
residuals	R; R_w 0.051; 0.051
goodness of fit indicator	1.49

Table 2. Intramolecular Bond Distances Involving the Non-Hydrogen Atoms of (DPPF)Pd[*p*-N(CH$_3$)$_2$C$_6$H$_4$][N(*p*-CH$_3$C$_6$H$_4$)$_2$] (**3b**)[a]

atom	atom	distance	atom	atom	distance
Pd	P1	2.283(2)	C13	C14	1.38(1)
Pd	P2	2.391(2)	C16	C17	1.41(1)
Pd	N1	2.097(7)	C16	C21	1.41(1)
Pd	C1	2.048(8)	C17	C18	1.39(1)
C1	C6	1.39(1)	C18	C19	1.40(1)
C2	C3	1.38(1)	C19	C20	1.36(1)
C3	C4	1.39(1)	C19	C22	1.53(1)
C4	C5	1.40(1)	C20	C21	1.39(1)
C5	C6	1.38(1)	C23	C24	1.42(1)
C9	C10	1.38(1)	N1	C9	1.39(1)
C9	C14	1.41(1)	N1	C16	1.374(9)
C10	C11	1.36(1)	N2	C4	1.40(1)
C11	C12	1.38(1)	N2	C7	1.45(1)
C12	C13	1.40(1)	N2	C8	1.45(1)
C12	C15	1.52(1)	C1	C2	1.40(1)

[a] Distances are in angstroms. Estimated standard deviations in the least significant figure are given in parentheses.

N atom of the amido ligand is planar; the sum of the three angles at nitrogen is 358.60°. The substituents at nitrogen are nearly orthogonal to the Pd square plane; the plane of the nitrogen forms a dihedral angle of 77.56° with the Pd square plane. The Pd−N distance is 2.10Å and falls in the range of M−N distances for other late metal arylamido complexes, despite the larger size of the diarylamido group.[44,45,59,68−70] The Pd-bound aryl group is also nearly orthogonal to the Pd square plane. In this case the dihedral angle between the aryl group and the square plane is 75.26°. The two Pd−P distances are different by over 0.1 Å. The Pd−P1 distance involving the phosphine trans to the amido ligand is 2.28 Å, while the Pd−P2 distance involving the phosphine trans to the aryl group is longer, 2.39 Å. The phosphorus−Cp(centroid)−Cp(centriod)−phosphorus tortional angle is 37.84°, which is large for ferrocene-based phosphine ligands and is presumably related to the large bite angle. The two Fe−centroid distances are both 1.64 Å.

4. Synthesis of a Palladium Azametallacycle. The metallacyclic amine complex *trans*-(PPh$_3$)Pd(C$_6$H$_4$C$_6$H$_4$NH$_2$)(I) (**4**) was prepared by oxidative addition of 2′-amino-2-iodobiphenyl

(62) This phosphine is commercially available. The ^{1}H NMR, GC retention time, and GC/MS were compared to an authentic commercial sample. In pp .

(63) Brown, J. M.; Guiry, P. J. *Inorg. Chim. Acta* **1994**, *220*, 249.

(64) Hayashi, T.; Konishi, M.; Kobori, Y.; Kumada, M.; Higuchi, T.; Hirotsu, K. *J. Am. Chem. Soc.* **1984**, *106*, 158.

(65) Butler, I. R.; Cullen, W. R.; Kim, T. J.; Retting, S. J.; Trotter, J. *Organometallics* **1985**, *4*, 972.

(66) Hayashi, T.; Kumada, M.; Higuchi, T.; Hirotsu, K. *J. Organomet. Chem.* **1987**, *334*, 195.

(67) Clemente, D. A.; Pilloni, G.; Coran, B.; Longato, B.; Tripicchio-Camellini, M. *Inorg. Chim. Acta* **1986**, *115*, L9.

(68) Hope, H.; Olmstead, M. M.; Murray, B. D.; Power, P. P. *J. Am. Chem. Soc.* **1985**, *107*, 712−713.

(69) Kolel-Veetil, M. K.; Rahim, M.; Edwards, J. A.; Rheingold, A. L.; Ahmed, K. J. *Inorg. Chem.* **1992**, *31*, 3877.

(70) Cowan, R. L.; Trogler, W. C. *J. Am. Chem. Soc.* **1989**, *111*, 4750.

Table 3. Selected Intramolecular Bond Angles Involving the Non-Hydrogen Atoms of (DPPF)Pd[*p*-N(CH_3)$_2$$C_6H_4$][N(*p*-$CH_3C_6H_4$)$_2$] (**3b**)[a]

atom	atom	atom	angle	atom	atom	atom	angle
P1	Pd	P2	100.47(9)	C25	Fe	C41	177.9(4)
P1	Pd	N1	171.9(2)	C25	Fe	C42	140.8(4)
P1	Pd	C1	84.9(2)	C25	Fe	C43	113.9(4)
P2	Pd	N1	87.6(2)	C25	Fe	C44	111.7(4)
P2	Pd	C1	174.4(2)	C26	Fe	C27	40.3(3)
N1	Pd	C1	87.0(3)	C26	Fe	C40	178.2(4)
Pd	P1	C45	113.7(3)	C1	C6	C5	121.9(8)
Pd	P1	C51	113.6(3)	N1	C9	C10	120.8(8)
C40	P1	C45	102.5(4)	N1	C9	C14	123.1(8)
C40	P1	C51	97.8(4)	C10	C9	C14	116.0(8)
C45	P1	C51	105.4(4)	C9	C10	C11	121.6(8)
Pd	P2	C23	116.9(3)	C10	C11	C12	123.6(9)
Pd	P2	C28	115.8(3)	C11	C12	C13	115.7(8)
Pd	P2	C34	113.1(3)	C11	C12	C15	124(1)
C23	P2	C28	102.1(4)	C13	C12	C15	120(1)
C23	P2	C34	104.9(4)	C12	C13	C14	121.5(9)
C28	P2	C34	102.3(4)	C9	C14	C13	121.6(9)
Pd	N1	C9	118.4(5)	N1	C16	C17	121.3(7)
Pd	N1	C16	117.8(5)	N1	C16	C21	121.7(8)
C9	N1	C16	122.4(7)	C17	C16	C21	116.9(8)
C4	N2	C7	118.3(8)	C16	C17	C18	120.5(8)
C4	N2	C8	118.7(8)	C17	C18	C19	121.8(8)
C7	N2	C8	113.0(8)	C18	C19	C20	117.5(9)
Pd	C1	C2	123.1(6)	C18	C19	C22	119.9(9)
Pd	C1	C6	121.2(6)	C20	C19	C22	123(1)
C2	C1	C6	115.6(7)	C19	C20	C21	122.4(9)
C1	C2	C3	123.0(8)	C16	C21	C20	120.9(8)

[a] Angles are in degrees. Estimated standard deviations in the least significant figure are given in parentheses.

Scheme 2

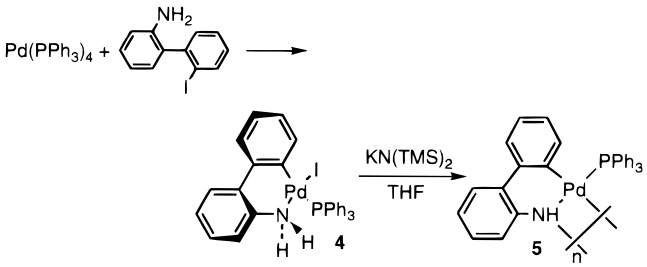

to $Pd(PPh_3)_4$ in benzene at 50 °C as shown in Scheme 2. The product precipitated out of solution as a beige solid during the course of the reaction and was isolated in 84% yield. The $^{31}P\{^1H\}$ NMR spectrum of **4** consisted of a singlet at δ 38.9 while the ^1H NMR spectrum at 50 °C contained a broad resonance centered at δ 5.13 for the two NH protons. Two NH resonances at δ 5.26 and δ 5.00 were observed in the ^1H NMR spectra obtained below 10 °C. This dynamic behavior is attributed to slow inversion of the ring-puckered structure in Scheme 2. Infrared vibrations at 3304 and 3233 cm^{-1} were observed for the two ν_{NH}.

Addition of $KN(TMS)_2$ to a THF or toluene solution of **4** generated the azametallacycle **5** as shown in Scheme 2. Complex **5** could not be isolated due to its reactivity at room temperature, but it was formed as the only transition-metal product that could be observed by NMR and was clearly identified in solution by NMR techniques. The formation of **5** was demonstrated by the appearance of a new resonance at δ 31.9 in the $^{31}P\{^1H\}$ NMR spectrum, an upfield shift of the NH resonance to δ 2.00 (d, J = 7.8 Hz), and a new NH band in the IR spectrum at 3298 cm^{-1}. The similarity of the N−H stretching frequency to that of a bridging palladium arylamido (*vide supra*)[59] and the reduced frequency from terminal arylamides,[37,40,41,70] along with the scarcity of three-coordinate Pd(II) species, suggests that the structure of **5** is dimeric.

Scheme 3

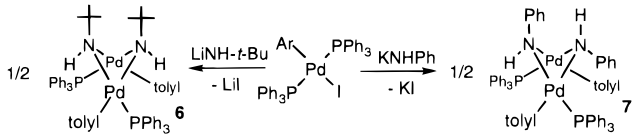

5. Dimeric Palladium Amido Complexes. The preparation of dimeric complexes [(PPh_3)Pd(*p*-$CH_3C_6H_4$)(μ-NH-*t*-Bu)]$_2$ (**6**) and [(PPh_3)Pd(*p*-$CH_3C_6H_4$)(μ-NHC_6H_5)]$_2$ (**7**) are summarized in Scheme 3. These complexes were prepared by addition of LiNH-*t*-Bu or KNHPh to *trans*-(PPh_3)$_2$Pd(*p*-$CH_3C_6H_4$)(I). On a small scale, addition of LiNH-*t*-Bu in THF led to formation of **6** in 60−80% yields by ^{31}P NMR spectroscopy (P(*o*-tolyl)$_3$ as internal standard) and the reaction to form **7** was similarly high yielding. However, isolation of **6** and **7** was hampered by similar solubility of the side product $Pd(PPh_3)_4$. Thus, pure samples of **6** and **7** were obtained by addition of 4-iodotoluene to crude reaction solutions to convert the soluble $Pd(PPh_3)_4$ to the sparingly soluble (PPh_3)$_2$Pd(*p*-$CH_3C_6H_4$)(I) and to allow for isolation of the amido complexes by crystallization. Analytically pure 6 and **7** were obtained by this procedure in 20% and 28% yields.

The NMR analysis of **6** and **7** indicated the rigid puckered structures in Scheme 3 for the two complexes. The $^{31}P\{^1H\}$ NMR spectrum of **6** contained one singlet at δ 25.7. Additionally, for the two amido ligands of **6** appeared in the ^1H NMR spectrum as a single resonance for the *t*-Bu protons (δ 1.3, s) and one doublet for the NH protons (δ −0.1, d, J = 5.3 Hz) coupled to a single phosphine ligand. The splitting of the NH resonance by a single phosphine ligand indicated that the phosphine ligands are oriented anti to one another. The presence of a single phosphine ^{31}P NMR signal and a single set of amido ^1H NMR signals for **6** indicates the geometry in Scheme 3. A ring-puckered geometry in which the alkyl groups of the amido ligands are oriented syn to each other or a geometry containing a planar Pd−N ring, with either syn or anti amido groups, would produce equivalent phosphine and amido groups.

The ^{31}P NMR spectrum of **7** contained two singlets at δ 29.69 and 29.73 for inequivalent phosphine ligands. The phosphine resonances for **7** coalesced upon heating a sample in the NMR probe at 95 °C. The ^1H NMR spectrum of **7**, however, contained two inequivalent NH resonances (δ 1.21, d, 4.3 Hz; 1.42, d, 5.3 Hz), each coupled to a single phosphine ligand. Again, the coupling of the NH resonances to a single phosphine required the phosphine ligands to possess an anti geometry. The inequivalence of the phosphine ligands and the doublet N−H signals reveal the geometry in Scheme 3 for **7**. The ring containing the two Pd and two N atoms is markedly puckered giving the molecule a "butterfly" configuration, and the NH protons are oriented anti to one another. This type of ring-puckered geometry has been previously observed for other dimeric bridging amido compounds.[44,50,55,71−73]

B. C−N-Bond-Forming Reductive Elimination of Amines. 1. C−N-Bond-Forming Reductive Elimination as a Cycliza-

(71) O'Mahoney, C. A.; Parkin, I. P.; Williams, D. J.; Woollins, J. D. *Polyhedron* **1989**, *8*, 1979.
(72) Alcock, N. W.; Bergamini, P.; Kemp, T. J.; Pringle, P. G. *J. Chem. Soc., Chem. Commun.* **1987**, 235.
(73) Park, S.; Roundhill, D. M.; Rheingold, A. L. *Inorg. Chem.* **1987**, *26*, 3972.
(74) Kong, K.; Cheng, C. *J. Am. Chem. Soc.* **1991**, *113*, 6313−6315.
(75) Reductive elimination and aryl group exchange are competing, but separate processes. Their dependence on ligand concentration identity is markedly different. Please see the following three references.
(76) Okeefe, D. F.; Dannock, M. C.; Marcuccio, S. M. *Tetrahedron Lett.* **1992**, *33*, 6679.
(77) Baranano, D.; Hartwig, J. F. *J. Am. Chem. Soc.* **1995**, *117*, 2937.
(78) Morita, D. K.; Stille, J. K.; Norton, J. R. *J. Am. Chem. Soc.* **1995**, *117*, 8576−8581.

Scheme 4

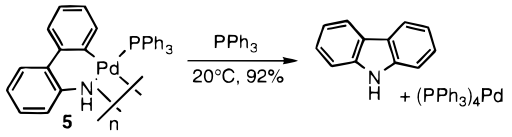

Scheme 5

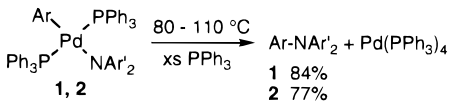

Scheme 6

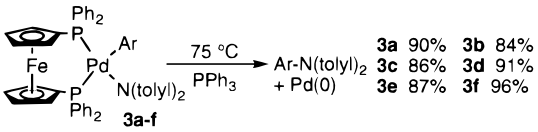

tion. Intramolecular reductive elimination reactions from the strained metallacycle **5** in Scheme 2 to form carbazole occurred at room temperature as shown in Scheme 4. Upon standing at room temperature for 1 h, **5** underwent C−N-bond-forming reductive elimination to give carbazole in 92% yield.

2. Reductive Elimination of Arylamine from Monomeric Palladium Amido Complexes 1 and 2. Heating of monomeric complexes **1** and **2**, in the presence of PPh_3, led to the reductive elimination of triarylamines (Scheme 5). The only palladium species observed by ^{31}P NMR spectroscopy at the end of the reaction was the palladium(0) triphenylphosphine complexes, which exist predominantly as a rapidly exchanging mixture of $Pd(PPh_3)_3$ and PPh_3.[79,80] Complex **1** formed NPh_3 in 84% yield upon heating in THF solvent at 80 °C for 5−12 h. Complex **2** produced $C_6H_5N(p\text{-}CH_3C_6H_4)_2$ in 77% yield after heating at 110 °C for 3−6 h in toluene-d_8 solution. In the absence of added phosphine, the yields of arylamine from **1** and **2** were less than 20%. Although the reaction was not fully investigated under these conditions, diarylamine and biphenyl were the major organic products. These reactions are among the first examples of C−N-bond-forming reductive elimination to form amine[59,60] and the first reductive elimination of a triarylamine.

3. Reductive Elimination of Amine from DPPF-Ligated Palladium Amido Complexes. The DPPF-ligated palladium aryl amido complexes **3a**−**f** underwent high-yielding (82−94%) reductive elimination reactions to form the corresponding triarylamine after 2−8 h at 75 °C in the presence of free PPh_3 as shown in Scheme 6.

We also observed reductive elimination reactions from DPPF-ligated complexes containing primary amido ligands as shown in Scheme 7. These primary amido complexes were not isolated, but were cleanly generated in solution. They underwent facile reductive eliminatoin of mixed secondary amines at room temperature or below. The addition of LiNH-*i*-Bu to a THF solution of (DPPF)Pd(Ph)(I) at 0 °C resulted in the formation of a new species which displayed two doublets in the $^{31}P\{^1H\}$ NMR spectrum (δ 26.5, 18.3; J = 22.0 Hz) and a new isobutyl group by ^1H NMR spectrometry. The ^{31}P chemical shifts of this product appeared downfield of those for (DPPF)-Pd(Ph)(I), in a similar manner to the downfield shifts of the resonances for **3a**. Given the clean reactivity of potassium amides with (DPPF)Pd(Ph)I to give **3a** and the similarity in chemical shifts, the reaction product formed at low temperature

Scheme 7

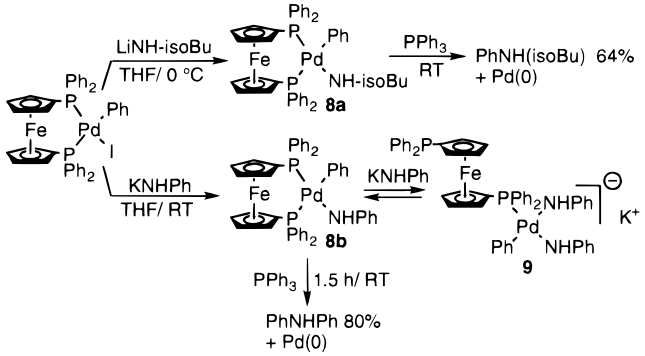

was assigned as the *cis*-ligated isobutylamido aryl complex **8a** shown in Scheme 7. Consistent with this proposal, PhNH-*i*-Bu was formed in 64% yield based on (DPPF)Pd(Ph)(I) upon warming a sample of **8a** to room temperature.

A new palladium amido complex **8b** was also formed upon addition of KNHPh to a THF solution of (DPPF)Pd(Ph)(I). The $^{31}P\{^1H\}$ NMR spectrum of this complex again contained two doublets at δ 25.1 and 6.3 (J = 38 Hz). To confirm the formation of a monomeric N-bound anilido complex, (DPPF)-Pd(Ph)(I) was reacted with [^{15}N]KNHPh to observe the $^{31}P-^{15}N$ couplings in **8b**. Coupling between the anilido ligand and each inequivalent phosphine was observed. The trans J_{NP} coupling was 43 Hz, while the *cis* coupling was 4 Hz. All of the coupling constants for the labeled compound are included in the Experimental Section. Anilido complex **8b** underwent reductive elimination of amine at or below room temperature. Ph−NHPh formed from **8b** in 80% yield after standing at room temperature for 1.5 h in the presence of added PPh_3.

During the course of our studies with KNHPh, we found that the addition of excess KNHPh reacted further with **8b** to form the complex **9**. The $^{31}P\{^1H\}$ NMR spectrum of **9** contained two singlets at δ 22.3 and −16.6, the upfield shift being similar to that of free DPPF. We had originally assigned **9** a dimeric structure containing bridging anilido groups.[32] However, complex **9-^{15}N** that was prepared from excess [^{15}N]KNHPh displayed a $^{31}P\{^1H\}$ NMR spectrum in which the downfield resonance exhibited $^{31}P-^{15}N$ coupling (δ 22.3, d, J_{NP} = 46 Hz) and displayed a $^{15}N\{^1H\}$ NMR spectrum in which two resonances (δ 86.5, d, J_{NP} = 46 Hz; 89.2, s) other than that for free [^{15}N]KNHPh were observed for inequivalent anilido ligands. The observation of inequivalent anilido ligands, only one of which is coupled to phosphorous, is inconsistent with a dimeric structure and is consistent with the structure for **9** in Scheme 7. Recently, related studies conducted on the reactivity of PPh_3- and DPPF-ligated palladium aryl halide complexes with KNC_4H_4 have also resulted in the isolation of some unusual anionic palladium bispyrrolyl complexes $X[(L)Pd(Ar)(NC_4H_4)_2]$ (X = K, NMe_4; L = PPh_3, η^1-DPPF), the chemistry of which will be reported elsewhere.[81]

4. Reductive Elimination Reactions of Dimeric Palladium Amido Complexes 6 and 7. In a similar fashion to the reactions of monomeric palladium amido complexes, the dimeric *tert*-butylamido complex **6** and the dimeric anilido complex **7** underwent C−N-bond-forming reductive elimination to form amine when heated in the presence of PPh_3 (Scheme 8). A toluene solution containing **6** and added PPh_3 formed (p-$CH_3C_6H_4$)NH-*t*-Bu in 90% yield upon heating for 8 h at 95 °C, while complex **7** formed $NHPh_2$ in 87% yield in the presence of PPh_3 after heating for 24 h at 95 °C. The palladium(0) triphenylphoshine complexes that rapidly equilibrate with PPh_3 were the only palladium species observed at the end of the

(79) (Triphenylphosphine)palladium, although $(PPh_3)_4Pd$ when isolated, is predominantly dissociated to $(PPh_3)_3Pd$ and free phosphine in solution: Amatore, C.; Pfluger, F. *Organometallics* **1990**, *9*, 2276−2282.

(80) Tolman C. A.; Seidel, W. C.; Gerlach, D. H. *J. Am. Chem. Soc.* **1972**, *94*, 2669.

(81) Driver, M. S.; Mann, G.; Hartwig, J. F. Manuscript in preparation.

Scheme 8

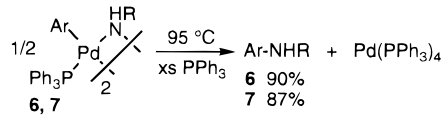

reaction by ^{1}H and ^{31}P{^{1}H} NMR spectroscopy. Again, the addition of PPh_3 to trap the Pd(0) species formed was essential for obtaining high yields of coupled amine product.

C. Mechanistic Investigation of the Reductive Elimination of Amines. 1. Mechanism of Reductive Elimination of Arylamine from 1 and 2. The formation of the C−N bond of amines from reactive metal−amido complexes is a key step in the catalytic formation of arylamines.[25−31] A clear description of how the reductive elimination of amines occurs will help the understanding of the chemistry of the active catalyst in the aryl halide amination process. This information has aided in the design of new catalysts with improved selectivity and activity.[32−34] We have studied in detail the mechanism of the C−N-bond-forming reductive elimination of arylamines from the palladium amido complexes described above.

Kinetic data for the reductive elimination of triphenylamine from **1** were obtained by monitoring the disappearance of **1** in THF solution by UV−vis spectroscopy. Complex **1** is red and has an absorption at $\lambda_{max} = 489.6$ nm ($\epsilon = 800$ cm^{-1} M^{-1}), which was used to monitor the concentration of **1** throughout the reaction. The products of the reaction did not show any absorption bands above 300 nm. The reactions were heated at 80 °C in sealed quartz cuvettes. UV−vis spectra were taken every 30 min. The reactions were conducted with [**1**] of 2.3 mM and [PPh_3] ranging from 22 to 68 mM to create pseudo-first-order conditions. Plots of ln (absorbance) vs time were linear over three half-lives, indicating a first-order dependence on [**1**]. By monitoring the reductive elimination at varied phosphine concentrations and graphing ln (k_{obs}) vs ln [PPh_3], an inverse first-order dependence of rate on [PPh_3] (slope $= -1.1 \pm 0.2$) was deduced. Unfortunately, this complex proved difficult to isolate reproducably in pure form, since it was typically obtained as powders. Further, the lack of well-resolved resonances in the ^{1}H NMR spectrum precluded simple analysis of its purity. Thus, we conducted a thorough study of the mechanism of the reductive elimination from diarylamido complexes using the *p*-tolyl analog **2**.

Complex **2** contains a tolyl methyl group that allowed for NMR spectroscopic monitoring of the reactions and allowed for assessment of the purity of different batches of amido complex without microanalytical data. Further, we found that these diarylamido complexes decomposed upon irradiation with a Hg arc lamp. Thus, a full study of the effect of phosphine concentration on the reaction rate was conducted by ^{1}H NMR spectroscopy using complex **2**.

Kinetic data for the reductive elimination of PhN(*p*-$CH_3C_6H_4)_2$ from **2** were obtained in toluene-d_8 solvent by monitoring the disappearance of the amidotolyl group by ^{1}H NMR spectroscopy. The reactions were conducted in the NMR probe at 110 °C; spectra were obtained at 1 min intervals. The reactions were conducted with [**2**] of 6.7 mM and [PPh_3] ranging from 52 to 470 mM to create pseudo-first-order conditions. Plots of ln [**2**] vs time were linear over three half-lives for all reaction conditions, again demonstrating a first-order dependence on [**2**]. The rate of reductive elimination was again inhibited by an increase in [PPh_3]. However, graphs of ln (k_{obs}) vs ln [PPh_3], which involved the higher reagent concentrations used in ^{1}H NMR spectroscopy as well as a wide range of [PPh_3], showed noninteger reaction orders between zero and one. This noninteger order was not observed with **1**. However, a smaller number of rate constants were measured in that case and they were measured within a smaller range of concentrations, most likely precluding our detection of a second pathway rather than indicating different chemistry between the two compounds.

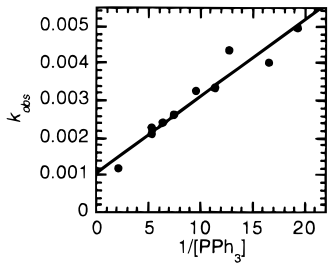

Figure 2. Plot of k_{obs} vs 1/[PPh_3] for the reductive elimination of di-*p*-tolylphenylamine from **2**. $R = 0.97$ for $y = (1.1 (\pm 0.2) \times 10^{-3} + [(2.1 (\pm 0.2) \times 10^{-4}]x$.

It seemed likely that the noninteger reaction order revealed in the studies with **2** resulted from competing processes that were zero and first order in [PPh_3]. A plot of k_{obs} vs 1/[PPh_3], which is given in Figure 2, is more informative. It revealed the two competing reaction pathways. This plot was linear with a positive slope and a positive, nonzero *y* intercept. The yields of triarylamine in these kinetic runs were not dependent on the changing [PPh_3]. Yields between 70% and 80% were observed for all reactions. These data show that two competing pathways exist for reductive elimination, one of which involves a monophosphine complex formed by phosphine dissociation and one of which involves a bis-phosphine complex. The detailed arguments for this conclusion are presented in the Discussion section.

2. Mechanism of Reductive Elimination from DPPF-Ligated Complexes 3a−f. According to the results in the previous section, *cis*-chelated complexes should eliminate triarylamine directly from the four-coordinate complex allowing us to obtain mechanistic data on the C−N-bond-forming reductive elimination in the absence of any competing processes. Kinetic data for the elimination of triarylamine from complexes **3a**−**f** were obtained by monitoring the disappearance of the palladium amido complex by ^{1}H NMR spectroscopy in toluene-d_8. The reactions were conducted in the NMR probe heated at 75 °C with spectra being obtained periodically. The reactions were conducted with a 13 mM concentration of palladium amido complex, and concentrations of PPh_3 ranging from 53 to 160 mM. The results of the kinetic analysis are summarized in Table 4. Plots of ln [**3a**−**f**] vs time were linear over three half-lives for all the complexes **3a**−**f**, demonstrating a first-order dependence, and the observed rate constants were independent of [PPh_3].

3. Electronic Effects on Reductive Elimination Reactions of DPPF-Ligated Palladium Amido Complexes 3a−f. Previous mechanistic studies conducted on the palladium-catalyzed amination of aryl halides have indicated the presence of a reactive palladium−amido intermediate and that the rates of catalysis were accelerated by aryl halides with electron-withdrawing substituents.[29] Also, electron-poor aryl halides often give higher yields of arylamine products in the catalytic amination, particularly for reactions of alkyl amines.[32,34] This enhanced yield is presumably due to an acceleration of the reductive elimination step of the catalytic cycle relative to competitive decomposition pathways, such as β-hydrogen elimination, which ultimately generates arene. A better understanding of the electronic influences on the reductive elimination reaction of amido complexes will help design of new catalysts for improved turnover numbers, substrate compatibility, and product selectivity, while providing fundamental information on an important class of reaction.

Table 4. k_{obs} for Reductive Elimination Reactions of **3a**−**f**

complex	conc (M)	[PPh_3] (M)	k_{obs} (s^{-1})
3a	0.013	0.11	29.4×10^{-4}
3b	0.013	0.11	2.5×10^{-4}
3c	0.013	0.11	2.1×10^{-4}
3d	0.013	0.11	13.8×10^{-4}
3e	0.013	0.11	35.2×10^{-4}
3f	0.013	0.11	43.3×10^{-4}

Table 5. k_{obs} for Reductive Elimination Reactions of **5** and **6**

complex	conc (M)	[PPh_3]	first order k_{obs} (s^{-1})	half order k_{obs}
6	0.0066	0.040	$7.2 \times 10^{-5} \pm .3$	−
6	0.0066	0.12	$7.2 \times 10^{-5} \pm .2$	−
6	0.015	0.12	$7.4 \times 10^{-5} \pm .2$	−
7	0.0058	0.092	$12.0 \times 10^{-6} \pm .1$	$1.2 \times 10^{-6} \pm .1$ $M^{0.5}$
7	0.023	0.092	$5.7 \times 10^{-6} \pm .2$	$1.0 \times 10^{-6} \pm .3$ $M^{0.5}$
7	0.0095	0.048	−	$1.4 \times 10^{-6} \pm .2$ $M^{0.5}$
7	0.0095	0.14	−	$1.6 \times 10^{-6} \pm .3$ $M^{0.5}$

Kinetic data for the reductive elimination of triarylamine from complexes **3a**−**f** were collected as described above and are summarized in Table 4. Indeed, we did observe an acceleration of C−N-bond-forming reductive elimination with complexes containing aryl groups with electron-withdrawing substituents. Complex **3f** with a *p*-Cl substituent reacted approximately 20 times faster than complex **3b** containing a *p*-OMe substituent, and the overall order of rate constants was *p*-Cl > *p*-SMe > *p*-H > *p*-Me > *p*-NMe_2 > *p*-OMe.

A qualitative comparison of the rates of reductive elimination for amido complexes with electronically different amido ligands was obtained by monitoring the elimination reactions of diarylamido complex **3a**, alkylamido **8a**, and anilide **8b**. The reductive elimination reaction was accelerated by electron-donating substituents on the nitrogen. Complex **8a**, containing an alkyl amido group, formed coupled amine rapidly at room temperature while **8b** took a couple of hours at room temperature to react fully. Complex **3a**, with a diaryl amido ligand, was stable at room temperature and reductively eliminated amine over several hours at 75 °C.

4. Mechanism of Arylamine Elimination from Dimeric 6 and 7. To compare the reactivities of the monomeric and dimeric palladium amido complexes, the mechanisms for the reductive elimination of amine from **6** and **7** were investigated. Kinetic data for the reductive elimination of (*p*-$CH_3C_6H_4$)NH-*t*-Bu from **6** in toluene-d_8 solution were obtained by monitoring the disappearance of the NH or the tolyl group Me resonance of **6** by ^{1}H NMR spectroscopy. The reactions were heated at 95 °C, and ^{1}H NMR spectra were obtained periodically. The reactions were conducted with [**6**] of either 4.3 mM or 10.3 mM and [PPh_3] of either 40.0 mM or 119 mM to create pseudo-first-order conditions. The results of the kinetic analysis are presented in Table 5. Plots of the ln [**6**] vs time were linear over three half-lives. Since it is difficult to distinguish half- and first-order reactions by the linearity of a $2 \times [\mathbf{6}]^{1/2}$ or ln [**6**] plot, we measured rate constants for reactions with different initial concentrations. The values of k_{obs} from the first-order plot were independent of the initial concentrations of **6**, indicating that the reaction is first order in palladium dimer **6**. The observed rate constants were also independent of phosphine concentration. Even at high [PPh_3], no evidence for monomeric, bis-phosphine palladium amido complexes was obtained during the reactions.

To probe for reversible dimer dissociation, reactions were conducted with a mixture of **6** and its phenyl analog [(PPh_3)-Pd(Ph)(μ-NH-*t*-Bu)]$_2$ (**6b**). If reversible cleavage of the dimeric complexes occurred during the reactions, then the mixed dimer [(PPh_3)(Ph)Pd(μ-NH-*t*-Bu)$_2$Pd(Tol)(PPh_3] (**6c**) would form during the reaction. Instead, no evidence for the formation of the mixed dimer **6c** was obtained over the course of the reaction. The *tert*-butyl resonances for **6**, **6b**, and **6c** can be distinguished by ^{1}H NMR spectroscopy at 50 °C.[82]

Kinetic data for the reductive elimination of diphenylamine from **7** in toluene-d_8 were obtained by monitoring the disappearance of an aromatic or NH resonance of **7** by ^{1}H NMR spectroscopy. The reactions were heated at 95 °C, and ^{1}H NMR spectra were obtained at 2 h intervals. The reactions were conducted with [**7**] between 5.9 and 22.4 mM and [PPh_3] between 47.7 mM and 143 mM to create pseudo-first-order conditions. The results of the kinetic analysis are summarized in Table 5. The observed rate constants for **7** were independent of [PPh_3]. The plots of $2 \times [\mathbf{7}]^{1/2}$ vs time were linear over three-half lives. Again, since half and first order reactions are difficult to distinguish by the linearity of a $2 \times [\mathbf{7}]^{1/2}$ or ln [**7**] plot, we measured rate constants for reactions with different initial concentrations. Plots of $2 \times [\mathbf{7}]^{1/2}$ gave comparable rate constants, k_{obs}, when initial concentrations of **7** were 5.9 mM and 22.4 mM, confirming that the reactions are half order in [**7**]. Furthermore, first-order plots for the decay of [**7**] (ln [**7**] vs time) produced rate constants that were proportional to the square root of the initial concentration of **7**, again indicating that the reaction has a half, rather than first, order dependence on [**7**].

Discussion

Reductive Elimination of Arylamine from Palladium Amido Complexes. Both the monomeric and dimeric palladium amido complexes produce arylamine by C−N-bond-forming reductive elimination. These isolable palladium amido complexes provide a means to model the reactivity of the palladium amido complexes proposed[27,29] in the catalytic formation of arylamine with discrete, well-characterized compounds. Although our complexes are the first examples of reductive elimination of triarylamines, a few other systems have been reported to undergo C−N-bond-forming reductive elimination to give amines.

The reactivity of some monomeric PMe_3-ligated complexes of the form *trans*-(PMe_3)$_2$Pd(R)(NHAr) (R = Me, Ph) have been studied.[59] When the complexes were heated at moderate temperatures (80 °C), phosphine dissociation occurred and dimeric amido complexes formed. Heating for longer times at higher temperature (110 °C) resulted in the slow reductive elimination of arylamine. In these studies, it was undetermined whether the reductive elimination reaction occurred from the monomeric or dimeric species. Some amido and azametallacycle complexes of Ni(II) have also been seen to eliminate arylamines.[60] In this case, reductive elimination was initiated by the addition of an oxidant to convert the Ni(II) to Ni(III). The formation of amine from Ni(III) was proposed to proceed through radical processes. There have also been reports of reductive elimination that form organic amides. In the Fe-facilitated synthesis of β-lactams, the final step in the synthesis involves the oxidation of the Fe center to promote C−N-bond-forming reductive elimination of the product.[83] Ni(II) amido complexes have also been seen to reductively eliminate organic amides upon reaction with CO,[61] although it is uncertain in this

(82) A sample of the mixed dimer was prepared by the reaction of (PPh_3)$_2$Pd(tol)I and (PPh_3)$_2$Pd(Ph)I with LiNH-*t*-Bu in THF, and it was analyzed by ^{31}P and ^{1}H NMR spectroscopy in C_6D_6. The ^{31}P NMR signals for the three compounds were not resolvable, but the ^{1}H NMR signals for the *t*-Bu peaks were distinguishable at 50 °C: **6a** δ 1.237 ppm; **6b** δ 1.218 ppm; **6c** δ 1.228 ppm and 1.226 ppm.

(83) Berryhill, S. R.; Price, T.; Rosenblum, M. *J. Org. Chem.* **1983**, *48*, 158−162.

Scheme 9

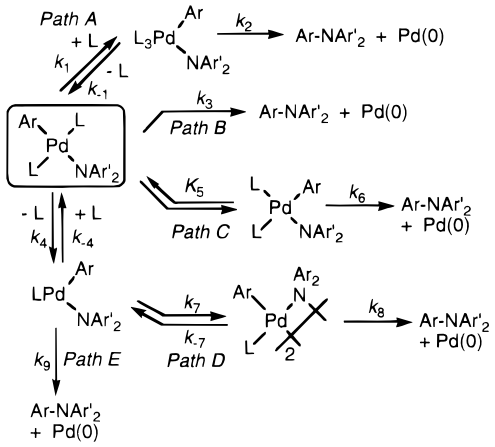

case whether the CO inserts into the Ni−R or Ni−NR_2 bond prior to reductive elimination.

Mechanism of Reductive Elimination from Monomeric Palladium Amido Complexes 1 and 2. Some of the possible mechanisms considered for the elimination of amine from **1** and **2** are provided in Scheme 9. Our kinetic data indicate two parallel pathways for reductive elimination from the PPh_3-ligated complexes, one of which dominates in the case of the PPh_3 complexes at low [PPh_3]. To begin the discussion on the mechanism of reductive elimination, we will first consider the kinetic data obtained for the monomeric PPh_3 complexes **1** and **2**. Our discussion will focus on the results for **2**, since the kinetic data for the reactions of this complex are most complete.

Pathway A consists of an associative mechanism in which PPh_3 coordinates to **2** to create a five-coordinate intermediate, which then reductively eliminates arylamine. This mechanism would result in the rate expression in eq 1.

$$\frac{-d[\mathbf{2}]}{dt} = k_{obs}[\mathbf{2}] \qquad (1)$$

$$k_{obs} = \frac{k_1 k_2 [PPh_3]}{k_{-1} + k_2}$$

This expression predicts a first order dependence on both [**2**] and [PPh_3]. Our kinetic data show an inverse first-order dependence on phosphine concentration ruling out pathway A.

Pathway B shows the mechanism for direct elimination of arylamine from the four-coordinate trans complex. This mechanism seems unlikely because earlier studies conducted on the reductive elimination of C−C and C−H bonds have determined that the ligands involved in bond formation need to be oriented cis to one another.[84−86] Yet, previous observations of C−N-bond-forming reductive elimination have suggested radical pathways[60] for the formation of amine, making pathway B worth consideration. The rate equation for pathway B is shown in eq 2 and would provide a first order dependence on [**2**] and no dependence on [PPh_3].

$$\frac{-d[\mathbf{2}]}{dt} = k_3[\mathbf{2}] \qquad (2)$$

Pathway C consists of a mechanism in which **2** isomerizes to a *cis*, four-coordinate complex, which then undergoes reductive elimination to form triphenylamine. Regardless of whether the isomerization occurs by phosphine association or dissociation, there is no net loss or gain of ligand before the rate determining step. Therefore, this pathway will show no rate dependence on [PPh_3]. The rate equation for this pathway is presented in eq 3.

$$\frac{-d[\mathbf{2}]}{dt} = k_{obs}[\mathbf{2}] \qquad (3)$$

where

$$k_{obs} = K_5 k_6$$

Trans-to-*cis* isomerization of related dialkyl complexes has been shown to occur at temperatures lower than those of the reductive elimination reactions, and reductive elimination reactions that do not occur by ionic pathways occur from *cis* complexes.

Pathway D shows an unusual dissociative mechanism in which a phosphine ligand is lost from **2** to generate a three-coordinate intermediate which then dimerizes. The dimeric complex then undergoes reductive elimination to produce triphenylamine. Although this mechanism seems unlikely, many isolated late-metal amido complexes have been dimeric(*vide supra*),[35,36,44,50,55,59,87] and these dimeric complexes do ultimately give amines by reductive elimination. In addition, previous observations of C−N-bond-forming reductive elimination indicated that amine formation occurred competitively with dimerization.[59] Pathway D would give rise to the rate expression in eq 4, which predicts a second-order dependence on [**2**] and an inverse second order dependence on [PPh_3].

$$\frac{-d[\mathbf{2}]}{dt} = k_{obs}[\mathbf{2}]^2 \qquad (4)$$

where

$$k_{obs} = \frac{k_4 k_7 k_8}{k_{-4} k_{-7} [PPh_3]^2 + k_{-4} k_8 [PPh_3]^2 + k_7 k_8}$$

Pathway E consists of a dissociative mechanism in which **2** reversibly loses a phosphine ligand to generate a three-coordinate intermediate that reductively eliminates arylamine. This mechanism would result in the rate expression in eq 5 where $k_9 << k_{-4}[PPh_3]$. Under these conditions, the rate expression predicts a first-order dependence on [**2**] and an inverse first-order dependence on [PPh_3].

Should two mechanisms occur simultaneously, then the overall rate equation will be the sum of the rate expressions for the two competing pathways. For example, should pathway C and E compete with each other, then the overall rate equation would be the one shown in eq 6.

$$\frac{-d[\mathbf{2}]}{dt} = k_{obs}[\mathbf{2}] \qquad (5)$$

where

$$k_{obs} = \frac{k_4 k_9}{k_{-4}[PPh_3] + k_9}$$

This rate equation can be simplified with the assumption that phosphine association is much faster than the actual C−N-bond-forming step. In this case, $k_9 << k_{-4}$. With this assumption, eq 6 simplifies to the expression in eq 7.

(84) Gillie, A.; Stille, J. K. *J. Am. Chem. Soc.* **1980**, *102*, 4933−4941.
(85) Sostero, S.; Traverso, O. *J. Organometal. Chem.* **1983**, *246*, 325−329.
(86) Ozawa, F.; Iro, T.; Nakamura, Y.; Yamamoto, A. *Bull. Chem. Soc. Jpn.* **1981**, *54*, 1868−1880.
(87) Casalnuovo, A. L.; Calabrese, J. C.; Milstein, D. *Inorg. Chem.* **1987**, *26*, 971−973.

$$\frac{-d[\mathbf{2}]}{dt} = k_{obs}[\mathbf{2}] \quad (6)$$

where

$$k_{obs} = K_5k_6 + \frac{k_4k_9}{k_{-4}[PPh_3] + k_9}$$

$$\frac{-d[\mathbf{2}]}{dt} = k_{obs}[\mathbf{2}] \quad (7)$$

where

$$k_{obs} = K_5k_6 + \frac{k_4k_9}{k_{-4}[PPh_3]}$$

In the case of both complexes **1** and **2**, the reductive elimination reactions were first order in [**2**] and inhibited by increasing [PPh_3]. Our results for **2** involve high [PPh_3] and a wide range of [PPh_3]. In this case, the graph of ln (k_{obs}) vs ln [PPh_3] was curved at high [PPh_3], indicating a change in the reaction order in phosphine as [PPh_3] was increased. However, the plot of k_{obs} vs 1/[PPh_3] was linear and displayed a positive slope and positive, nonzero intercept. The positive slope of this plot reveals one reaction pathway that is inverse first order in [PPh_3]. The nonzero intercept reveals a competing pathway that is independent of [PPh_3]. In other words, this plot corresponds to eq 7, the equation for two competing pathways, one of which is independent of [PPh_3] and one of which is inversely dependent on [PPh_3]. The pathway that shows inverse first-order dependence on [PPh_3] is path E, the pathway in which C−N bond formation occurs within a three-coordinate 14-electron intermediate. The pathway that is independent of [PPh_3] could be path B, the direct elimination from the isolated *trans* isomer, or path C, elimination from the four-coordinate, 16-electron *cis* isomer. It is most reasonable that C−N bond formation occurs from the *cis* isomer. We have obtained no evidence for radical pathways and amide dissociation is unlikely considering the nonpolar solvent and the absence of a substantial solvent effect. Previous concerted reductive eliminations are well known and require a *cis* arrangement of ligands. *Thus, at low [PPh_3], reductive elimination from the three-coordinate intermediate is the primary pathway for formation of triarylamine (pathway E); however, as [PPh_3] is increased, pathway C through the cis, four-coordinate intermediate contributes substantially to the total rate. This information on PPh_3-ligated complexes clearly implies that the pathway for reductive elimination of amine from an amido complex containing a chelating ligand will involve a four-coordinate intermediate.*

Comparison of C−N Bond Formation to C−H-, C−C-, C−S-, and C−O-Bond-Forming Reductive Eliminations. Similar kinetic results were obtained for the reductive elimination of carborane from the complex *trans*-(PPh_3)$_2$(CO)Ir(σ-carb)-(H)Cl.[88,89] For this system, the reductive elimination occurred primarily via phosphine dissociation to give a five-coordinate intermediate which eliminated carborane. However, at high [PPh_3], the five-coordinate intermediate competitively underwent isomerization and reassociation of phosphine ligand to give the *cis*-oriented six-coordinate complex which eliminated carborane. For square-planar complexes, C−H-bond-forming reductive eliminations are believed to occur predominantly from four-coordinate species.

Previous studies conducted on square-planar, d^8 metal complexes have shown the presence of dissociative mechanisms for C−C-bond-forming reductive elimination reactions. The series of studies conducted on the reductive elimination of ethane from both *cis*- and *trans*-(PPh_2R)$_2$PdR′$_2$ (R = Ph, Me; R′ = Me, Et) have shown that initial phosphine dissociation is required for reductive elimination.[84,86] The Au(III) complex (PPh_3)$AuMe_3$ must also lose its phosphine ligand before the reductive elimination of ethane.[90] The reductive elimination of 1,1-dimethylcyclopropane is thought to proceed via ligand dissociation from the platinocyclobutane (P-*i*-Pr_3)$_2$Pt($CH_2C(CH_3)_2$-CH_2).[89]

Nevertheless, some reductive elimination reactions to form C−C bonds have been observed directly from four-coordinate complexes. In Stille's studies,[84] reductive elimination of ethane occurred from complexes containing chelating phosphines, but with rates that were approximately 100 times slower than those with monodentate ligands. In studying palladium-catalyzed C−C cross-coupling reactions, Hayashi found that the presence of chelating ligands inhibits decompostion pathways such as β-hydrogen elimination and leads to high yields of coupled product via reductive elimination.[82] Of course, it is difficult to determine in the reactions of complexes with chelating ligands whether the bis-phosphine undergoes reductive elimination or whether dissociation of an arm of the chelate occurs before reductive elimination. Stang and Young have reported rates for C−C-bond-forming reductive elimination from platinum vinyl alkynyl and diaryl complexes that are either independent of [PPh_3] or slightly accelerated by added PPh_3. These results could indicate either elimination without phoshine dissociation or irreversible phosphine dissociation. Our kinetic results for complexes with monodentate ligands explicitly show that two reaction pathways are followed for the reductive elimination of arylamines, one through a three-coordinate monophosphine complex and one through a four-coordinate bisphosphine complex.

The reductive elimination to form a carbon−heteroatom bond from four-coordinate complexes has previously been observed for the formation of sulfides from (DPPE)Pd(Ar)(SR).[77] To test whether dechelation was occurring, analogous thiolate complexes with more rigid chelating ligands were studied. The DPPE, bis(diphenylphosphino)benzene, and bis(diphenylphosphino)ethene complexes all eliminated at similar rates, and these rates were slower than the extremely rapid rates for reductive elimination from three-coordinate 14-electron monophoshine thiolates generated from tin thiolates.[92] Thus, a rapid elimination from the unsaturated intermediate and slower elimination from a four-coordinate intermediate, again, appears to occur. C−O-bond-forming reductive eliminations of esters has been observed by Yamamoto, and these reactions occur by reductive elimination from both three- and four-coordinate complexes.

Mechanism of Reductive Elimination of Arylamine from DPPF-Ligated Complexes. The kinetic data for reductive elimination from complexes **3a**−**f** demonstrate that the reductive elimination reaction is first order in the palladium amido complex. The observed rate constants were also independent of [PPh_3], again ruling out an associative mechanism for the reductive elimination. The added phosphine serves only as a trap for the Pd(0) fragment formed after reductive elimination of amine. These data are consistent with our hypothesis that reductive elimination of triarylamine from the DPPF-ligated palladium amido complexes occurs directly from the four-coordinate complex.

Electronic Effects on the Reductive Elimination of Aryl-

(88) Basato, M.; Morandini, F.; Longato, B.; Bresadola, S. *Inorg. Chem.* **1984**, *23*, 649−653.

(89) carb = 7-C_6H_5-1,7-$C_2B_{10}H_{10}$.

(90) Komiya, S.; Albright, T. A.; Hoffman, R.; Kochi, J. K. *J. Am. Chem. Soc.* **1976**, *98*, 7255.

(91) DiCosimo, R.; Whitesides, G. M. *J. Am. Chem. Soc.* **1982**, *104*, 3601.

(92) Louie, J.; Hartwig, J. F. *J. Am. Chem. Soc.* **1995**, *117*, 11598.

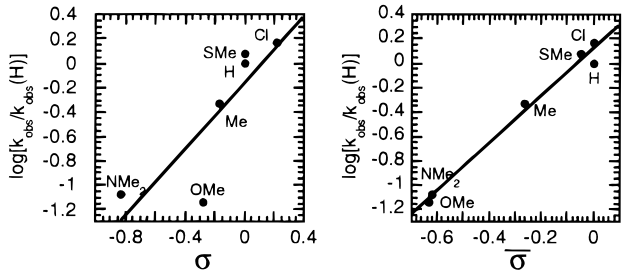

Figure 3. Free energy relationships for the C−N-bond-forming reductive elimination reactions of **3a**−**f**. The left plot shows $\log(k_{obs}/k_{obs}(H))$ vs σ; the right plot shows $\log(k_{obs}/k_{obs}(H))$ vs $\bar{\sigma}$.

amine. The relative rates for reductive elimination of **3a**−**f** directly probe the electronic properties of the transition state because reductive elimination occurs from the observed four-coordinate complex without any preceding ligand dissociation or isomerization. The plot on the left of Figure 3 shows that the substituent effects do not follow a simple linear free-energy relationship with the σ values derived from the acidity of substituted benzoic acids. Similar results were also observed in the case of sulfide reductive elimination from (DPPE)Pd(Ar)(SR). The separation of the resonance and inductive σ effects has been previously described for reactions of organic compounds.[93,94] In this treatment, a synthetic σ value ($\bar{\sigma}$) is constructed from separate resonance and inductive σ values. A σ generated from weighting the resonance effect more than the inductive effect ($\bar{\sigma} = 2\sigma_R + \sigma_I$) provides the best fit to our data for elimination of amines from Pd(II). The plot of log (k_{obs}) vs σ is shown on the right of Figure 3. Although a small number of points are used in the analysis of this paper, an identical effect was observed in the reductive elimination of sulfides that involved 11 different substituents. Thus, it appears to be a general result for C−X-bond-forming reductive elimination from palladium complexes that resonance effects dominate over inductive effects, although we draw no quantitative conclusions from the data of the amido complexes. An analysis of Yamamoto's previous data[95] for formation of sp^2−sp^3 C−C-bonds from Pd(II) also reveals that resonance effects are more important than inductive effects in this reaction. In the case of C−C- and C−H-bond-forming reductive eliminations, theoretical studies have indicated that the reactions are accelerated by electron-donating substituents.[96] In the case of bond formation involving sp^2-hybridized carbon atoms this predicted trend is clearly not observed. More recently, Calhorda[95] has provided a theoretical study on bond formation involving vinyl groups that may be more relevant.

Our qualitative studies conducted with varied amido ligands is consistent with the results of the electronic effects of the aryl substituents. Since electron-withdrawing substituents on the aryl ligand accelerate reductive elimination, it is reasonable that a complementary effect from the amido group—electron-donating substituents accelerating reductive elimination—would be observed. The overall reactivity of the amido groups was diarylamido < arylamido < alkylamido. This trend shows that electron-donating groups accelerate reductive elimination in this case. In other words, the amido group acts as a nucleophile, and the aryl group acts as an electrophile.

Mechanism of Reductive Elimination from Dimeric Palladium Amido Complexes 6 and 7. Some possible mechanisms considered for the elimination of amine from **6** are shown in Scheme 10. Pathway A consists of a mechanism involving phosphine association which acts to cleave the palladium dimer and form one three- and one four-coordinate monomeric species, one or the other of which reductively eliminates amine product. This mechanism would give the rate expression shown in eq 8 which predicts a half-order dependence on [**6**] and a first order dependence on [PPh_3].

Scheme 10

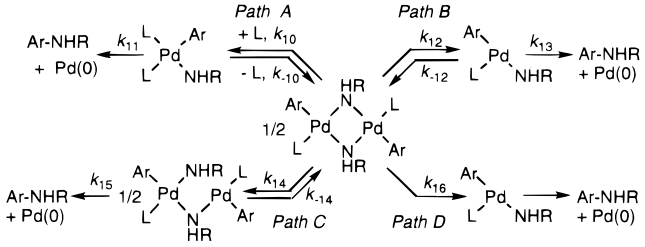

$$\frac{-d[\mathbf{6}]}{dt} = k_{obs}[\mathbf{6}]^{1/2} \tag{8}$$

where

$$k_{obs} = \frac{k_{10}k_{11}[PPh_3]}{k_{-10} + k_{11}}$$

Our kinetic data show a first-order dependence on [**6**] and no dependence on [PPh_3], ruling out the associative mechanism of pathway A.

Pathway B shows a mechanism consisting of reversible dimer cleavage to generate a three-coordinate intermediate, which eliminates amine product. This mechanism would result in the rate expression in eq 9 giving a half-order dependence on [**6**] and no dependence on [PPh_3].

$$\frac{-d[\mathbf{6}]}{dt} = k_{obs}[\mathbf{6}]^{1/2} \tag{9}$$

where

$$k_{obs} = \frac{k_{12}k_{13}}{k_{-12} + k_{13}}$$

This mechanism would also result in formation of the mixed dimer **6c** from the thermolysis of the mixture of **6** and **6b**. Reversible dimer cleavage is inconsistent with the observed first-order dependence on [**6**] and absence of the cross-over product **6c**.

Pathway C involves partial cleavage of the dimeric **6** to form a complex containing one three- and one four-coordinate palladium. This intermediate complex could be formed reversibly or irreversibly from **6**. In either case, the rate of the reductive elimination process would be first order in [**6**] and zero order in [PPh_3] as shown in the rate expression in eq 10.

$$\frac{-d[\mathbf{6}]}{dt} = k_{obs}[\mathbf{6}] \tag{10}$$

where

$$k_{obs} = \frac{k_{14}k_{15}}{k_{-14} + k_{15}}$$

This pathway would also predict the absence of the mixed dimer **6c** during the course of the reductive elimination. Although the intermediate in this pathway is perhaps counterintuitive, it

(93) Wells, P. R.; Ehrenson, S.; Taft, R. W. *Prog. Phys. Org. Chem.* **1969**, *6*, 147.
(94) Ehrenson, S.; Brownlee, R. T. C.; Taft, R. W. *Prog. Phys. Org. Chem.* **1973**, *10*, 1.
(95) Ozawa, F.; Kurihara, K.; Fujimori, M.; Hidaka, T.; Toyoshima, T.; Yamamoto, A. *Organometallics* **1989**, *8*, 180−188.
(96) Tatsumi, K.; Hoffman, R.; Yamamoto, A.; Stille, J. K. *Bull. Chem. Soc. Jpn.* **1981**, *54*, 1857−1867.

is likely to be an intermediate in the cleavage of dimeric amido complexes and its intermediacy in the reductive elimination process is consistent with the first-order behavior in [**6**], zero-order behavior in [PPh_3], and the absence of mixed dimer **6c** during the reaction.

However, pathway D is also consistent with these data. Pathway D consists of a mechanism involving irreversible dimer cleavage to give a three-coordinate intermediate. The three-coordinate complex then undergoes rapid reductive elimination of amine. This pathway would result in the rate expression shown in eq 11 that contains a first-order dependence on [**6**] and no dependence on [PPh_3].

$$\frac{-d[\mathbf{6}]}{dt} = k_{16}[\mathbf{6}] \qquad (11)$$

This mechanism also predicts the absence of the mixed dimer **6c**. Although it seems more likely that full cleavage of **6** preceded elimination, we sought firm data that the dimeric complexes fully cleaved to monomers before reductive elimination.

The PPh_3-ligated anilido complexes underwent reductive elimination more slowly than the alkyl amido complexes. Qualitatively, reductive elimination of amine from **6** was much faster than reaction of **7** (8 h vs 24 h at 95 °C). This slower reactivity of **7** is most likely due to slower reductive elimination since **7** contains the less electron-rich anilido ligand. Thus, the dimer cleavage is more likely to be reversible in the case of anilido complex **7**. The kinetic data for the reductive elimination from **7** did reveal reversible dimer cleavage to form two monomeric, three-coordinate 14-electron intermediates. The rate of the reductive elimination was half order in [**7**] and independent of [PPh_3]. *These kinetic data are inconsistent with pathway C involving incomplete dimer cleavage, and are consistent with only pathway B involving reversible dimer dissociation to form a three-coordinate intermediate which then undergoes C−N-bond-forming reductive elimination to give amine product*. As a result, reaction of the *tert*-butylamido dimer by pathway D involving full dimer cleavage, rather than pathway C involving partial dimer cleavage, is almost certainly followed for the elimination from the alkylamido dimer **6**. Thus, the dimeric complexes undergo C−N-bond-forming reductive eliminations through the same three-coordinate intermediates that dominate the chemistry of the PPh_3-ligated monomeric diarylamido complexes at low [PPh_3].

Conclusions

A series of monomeric and dimeric palladium amido complexes have been prepared which undergo C−N-bond-forming reductive elimination to form amines when heated. Using PPh_3-ligated palladium amido complexes **1** and **2**, the presence of two concurrent mechanisms for the reductive elimination of amine were detected. At low [PPh_3], a mechanism involving phosphine dissociation to generate a three-coordinate intermediate which then eliminates amine is the primary pathway for reductive elimination. As [PPh_3] is increased, this dissociative pathway is inhibited, and a mechanism involving reductive elimination from a four-coordinate complex dominates. These results led to the preparation of a series of DPPF-ligated palladium amido complexes which reductively eliminated amine directly from the *cis*, four-coordinate palladium amido complex. Using these DPPF-ligated complexes, we observed that the reductive elimination reaction is accelerated by electron-withdrawing substituents of the palladium-bound aryl ring and that the resonance effects (σ_R) were more substantial than the inductive effects (σ_I). We were also able to observe high-yielding reductive elimination of mixed arylamines from a DPPF-ligated palladium primary alkylamido complex. The dimeric palladium amido complexes **6** and **7** also underwent C−N-bond-forming reductive elimination. The mechanism of reductive elimination of the dimeric complexes involved dimer dissociation to generate two three-coordinate intermediates that were analogous to those formed by the PPh_3-ligated monomeric amido complexes. In the case of the alkyl amido dimer **6**, dimer cleavage was irreversible while for the anilido dimer **7**, dimer dissociation was reversible due to the presence of the electron-withdrawing anilido group.

Experimental Section

General Methods. Unless otherwise noted, all reactions and manipulations were performed in an inert atmosphere glovebox or by using standard Schlenk techniques. All $^{31}P\{^1H\}$ NMR chemical shifts are reported in parts per million relative to an 85% H_3PO_4 external standard. Shifts downfield of the standard are reported as positive. Benzene, toluene, THF, ether, and pentane solvents were distilled from sodium/benzophenone prior to use. Triphenylphosphine was sublimed prior to use in kinetic reactions. *trans*-$(PPh_3)_2Pd(Ar)I$[98] was prepared according to literature procedures. All other chemicals were used as received from commercial suppliers.

Preparation of *trans*-$[P(C_6H_5)_3]_2Pd(C_6H_5)[N(C_6H_5)_2]$ (1). Into a 20 mL vial was weighed 105 mg of $[P(C_6H_5)_3]_2Pd(C_6H_5)(I)$ (0.126 mmol). This material was suspended in 12 mL of THF and 27 mg of $KN(C_6H_5)_2$ (0.13 mmol) was added to the suspension as a solid. The reaction mixture was stirred for 30 min at room temperature and turned a deep red color. The reaction mixture was filtered through a medium fritted funnel. The resulting THF solution was concentrated under vacuum. Crystalline material was obtained by layering with Et_2O and cooling at −35 °C. The yield of red crystalline product was 93 mg (84%). ^1H NMR: (C_6D_6) δ 6.26 (d, 7.6 Hz, 1H), 6.62 (t, 7.1 Hz, 1H), 6.80−6.92 (m, 21H), 7.06 (t, 7.7 Hz, 4H), 7.43 (d, 7.2 Hz, 4H), 7.47−7.56 (m, 12H), 7.71−7.75 (m, 2H). $^{31}P\{^1H\}$ NMR: (THF) δ 21.4. IR (cm^{-1}): (KBr) 3052 (m), 2991 (w), 2921 (m), 2849 (m), 1574 (s), 1468 (s), 1433 (s) 1313 (s) 1218 (m), 1170 (m), 1095 (s), 987 (m), 791 (s), 741 (s), 691 (s). UV−vis: (THF) λ_{max} = 489.6 nm (ϵ = 880 cm^{-1} M^{-1}). Anal. Calcd for $C_{54}H_{45}NP_2Pd$: C, 74.01; H, 5.18; N, 1.60. Found: C, 73.46; H, 5.55; N, 1.50.

Preparation of *trans*-$[P(C_6H_5)_3]_2Pd(C_6H_5)[N(p\text{-}CH_3C_6H_4)_2]$ (2). Into a 20 mL vial was weighed 218 mg (0.261 mmol) of *trans*-$(PPh_3)_2$-Pd(Ph)(I). The material was suspended in 15 mL of THF and 68 mg (0.289 mmol) of $KN(p\text{-}CH_3C_6H_4)_2$ was added as a solid. The reaction mixture was stirred for 1 h at room temperature and turned a deep red color. The reaction mixture was filtered through a medium fritted funnel. The resulting THF solution was concentrated by vacuum. Crystalline material was obtained by addition of Et_2O and cooling at −35 °C for 12 h. The yield of red crystalline product was 184 mg (78%). ^1H NMR: (C_6D_6) δ 2.26 (s, 6H), 6.40 (t, 8.3 Hz, 2H), 6.52 (t, 7.1 Hz, 1H), 6.86 (d, 8.3 Hz, 4H), 6.91−7.01 (m, 20 H), 7.39 (d, 8.3 Hz, 4H), 7.50−7.56 (m, 12H). $^{13}C\{^1H\}$ NMR: (C_6D_6) δ 20.7 (s), 120.0 (s), 121.5 (s), 122.4 (s), 126.2 (s), 127.7 (s), 128.5 (s), 129.4 (s), 131.4 (t, 21.9 Hz), 134.5 (t, 6.0 Hz), 140.0 (t, 3.8 Hz), 149.2 (t, 7.0 Hz), 156.6 (s). $^{31}P\{^1H\}$ NMR: (toluene) δ 21.0 (s). Anal. Calcd for $C_{56}H_{49}N_1P_2Pd$: C, 74.37; H, 5.46; N, 1.55. Found: C, 74.18; H, 5.66; N, 1.38.

General Procedure for the Preparation of (DPPF)Pd(Ar)X. (DPPF)Pd(Ph)(I).[63] *trans*-$(PPh_3)_2Pd(Ph)(I)$ (302 mg, 0.362 mmol) was suspended in 4 mL of THF. DPPF (221 mg, 0.399 mmol) was added to the stirred suspension as a solid. The reaction was allowed to stir at room temperature for 30 min. The product was precipitated by the addition of 15 mL of pentane. The product was collected as a solid by filtration on a fritted glass funnel to yield 272 mg (87%). The product was used without further purification.

Preparation of (DPPF)Pd(p-$CH_3OC_6H_4$)(I). Using the general procedure with 250 mg (0.289 mmol) of *trans*-$(PPh_3)_2Pd(p\text{-}CH_3OC_6H_4)$-(I) and 176 mg (0.318 mmol) of DPPF gave 201 mg (78%) of product.

(97) Calhorda, M. J.; Brown, F. M.; Cooley, N. A. *Organometallics* **1991**, *10*, 1431−1438.

(98) Fitton, P.; Johnson, M. P.; McKeon, J. E. *J. Chem. Soc., Chem. Commun.* **1968**, 6−7.

^{1}H NMR: (C_6D_6) δ 3.28 (s, 3H), 3.66 (m, 2H), 3.71 (m, 2H), 3.93 (m, 2H), 4.53 (m, 2H), 6.44 (d, 6.7 Hz, 2H), 6.80−7.09 (m, 14H), 7.40−7.46 (m, 4H), 8.34−8.39 (m, 4H). ^{31}P{^{1}H} NMR: (C_6D_6) δ 29.4 (d, 32.4 Hz), 8.9 (d, 32.4 Hz).

Preparation of (DPPF)Pd(*p*-$CH_3C_6H_4$)(I). Using the general procedure with 248 mg (0.292 mmol) of *trans*-$(PPh_3)_2$Pd(*p*-$CH_3C_6H_4$)-(I) and 178 mg (0.321 mmol) of DPPF gave 208 mg (81%) of product. ^{1}H NMR: (C_6D_6) δ 2.04 (s, 3H), 3.65 (m, 2H), 3.72 (m, 2H), 3.93 (m, 2H), 4.50 (m, 2H), 6.52 (d, 6.6 Hz, 2H), 6.81−7.12 (m, 14H), 7.39−7.45 (m, 4H), 8.28−8.34 (m, 4H). ^{31}P{^{1}H} NMR: (C_6D_6) δ 25.1 (d, 34.8 Hz), 8.0 (d, 34.8 Hz).

Preparation of (DPPF)Pd(*p*-$CH_3SC_6H_4$)(Br). Using the general procedure with 260 mg (0.309 mmol) of *trans*-$(PPh_3)_2$Pd(*p*-$CH_3SC_6H_4$)-(I) and 188 mg (0.340 mmol) of DPPF gave 218 mg (81%) of product. ^{1}H NMR: ($CDCl_3$) δ 3.72 (m, 2H), 4.16 (m, 2H), 4.50 (m, 2H), 4.66 (m, 2H), 6.55 (d, 6.7 Hz, 2H), 6.84−6.89 (m, 2H), 7.15−7.26 (m, 4H), 7.34−7.50 (m, 12H), 8.01−8.05 (m, 4H). ^{31}P{^{1}H} NMR: (C_6D_6) δ 29.4 (d, 33.0 Hz), 9.2 (d, 33.0 Hz).

Preparation of (DPPF)Pd(*p*-ClC_6H_4)(I). Using the general procedure with 240 mg (0.276 mmol) of *trans*-$(PPh_3)_2$Pd(*p*-ClC_6H_4)(I) and 168 mg (0.304 mmol) of DPPF gave 226 mg (91%) of product. ^{1}H NMR: ($CDCl_3$) δ 2.28 (s, 3H), 3.64 (m, 2H), 4.16 (m, 2H), 4.50 (m, 2H), 4.68 (m, 2H), 6.60 (d, 7.3 Hz, 2H), 6.86−9.82 (m, 2H), 7.13−7.18 (m, 4H), 7.29−7.50 (m, 12H), 8.03−8.10 (m, 4H). ^{31}P{^{1}H} NMR: (C_6D_6) δ 25.2 (d, 33.0 Hz), 8.7 (d, 33.0 Hz).

Preparation of (DPPF)Pd(*p*-$NMe_2C_6H_4$)(Br). {[P(*o*-tolyl)$_3$](*p*-$NMe_2C_6H_4$)Pd(μ-Br)}$_2$[27] (240 mg, 0.197 mmol) was suspended in 4 mL of THF. DPPF (240 mg, 0.433 mmol) was added to the stirred suspension as a solid. The reaction was allowed to stir at room temperature for 10 min. The product was precipitated by the addition of 15 mL of pentane. The product was collected as a solid by filtration on a fritted glass funnel to yield 281 mg (83%). The product was used without further purification. ^{1}H NMR: (C_6D_6) δ 2.46 (s, 6H), 3.67 (m, 2H), 3.74 (m, 2H), 3.93 (m, 2H), 4.53 (m, 2H), 6.30 (d, 7.0 Hz, 2H), 6.85−7.06 (m, 14H), 7.44−7.50 (m, 4H), 8.35−8.41 (m, 4H). ^{31}P{^{1}H} NMR: (C_6D_6) δ 29.2 (d, 33.6 Hz), 8.5 (d, 33.6 Hz).

Preparation of (DPPF)Pd(C_6H_5)[N(*p*-$CH_3C_6H_4$)$_2$] (3a). (DPPF)-Pd(C_6H_5)(I) (174 mg, 0.201 mmol) was suspended in 15 mL of toluene. KN(*p*-$CH_3C_6H_4$)$_2$ (52 mg, 0.221 mmol) was added to the solution as a solid. The reaction was stirred at room temperature for 30 min, and it turned a deep red color. The reaction mixture was filtered through Celite, and the toluene was removed under vacuum. The resulting solid was dissolved in 8 mL of THF. The THF solution was concentrated under vacuum and layered with Et_2O. Pure crystalline material was obtained by cooling the layered solution at −35 °C for 12 h. The yield of **3a** was 129 mg (69%). ^{1}H NMR: (C_6D_6) δ 2.23 (s, 6H), 3.72 (m, 2H), 3.94 (m, 2H), 4.15 (m, 2H), 4.48 (m, 2H), 6.55 (m, 3H), 6.89 (d, 8.2 Hz, 4H), 7.00−7.06 (m, 14H), 7.32 (d, 8.2 Hz), 4H, 7.65 (m, 4H), 7.83 (m, 4H). ^{13}C{^{1}H} NMR: (C_6D_6) δ 20.98 (s), 72.22 (d, 6.1 Hz), 73.38 (d, 5.6 Hz), 73.85 (d, 34.1 Hz), 74.98 (d, 8.9 Hz), 75.56 (d, 11.3 Hz), 78.97 (dd, 41.3 Hz, 8.9 Hz), 121.98 (s), 123.45 (s), 126.25 (d, 8.8 Hz), 127.51 (d, 9.1 Hz), 127.81 (d, 9.6 Hz), 128.05 (s), 128.62 (s), 129.91 (s), 129.91 (s), 132.89 (d, 49.9 Hz), 134.45 (d, 11.8 Hz), 135.15 (d, 12.9 Hz), 135.26 (d, 34.2 Hz), 136.40 (s), 153.30 (s), 158.80 (dd, 121.2 Hz, 8.1 Hz). ^{31}P{^{1}H} NMR: (THF) δ 23.5 (d, 35.4 Hz), 14.9 (d, 35.4 Hz). IR (cm^{-1}): (KBr) 3051 (m), 3010 (m), 2908 (m), 2854 (m), 1598 (s), 1566 (s), 1549 (s), 1490 (s), 1432 (m), 1389 (s), 1314 (s), 1292 (m), 1259 (s), 1219 (s), 1200 (w), 1170 (w), 1098 (m), 1063 (s), 1016 (s), 995 (m), 899 (w), 886 (w), 866 (m), 839 (m), 829 (m), 809 (s), 799 (s), 772 (s), 746 (s), 728 (s), 691 (m), 638 (w), 631 (w), 587 (w), 565 (m), 540 (s), 514 (s), 488 (m), 159 (m). Anal. Calcd for $C_{54}H_{47}FeNP_2Pd$: C 69.43, H 5.07, N 1.50. Found: C 69.18, H 4.93, N 1.25.

Preparation of (DPPF)Pd(*p*-$NMe_2C_6H_4$)[N(*p*-$CH_3C_6H_4$)$_2$] (3b). Following the procedure for the preparation of **3a**, (DPPF)Pd(*p*-$NMe_2C_6H_4$)(Br) (180 mg, 0.209 mmol) was reacted with KN(*p*-$CH_3C_6H_4$)$_2$ (52 mg, 0.221 mmol) in THF. Recrystallization at −35 °C from a concentrated THF solution layered with ether gave 159 mg of pure **3b** (78%). ^{1}H NMR: (C_6D_6) δ 2.24(s, 6H), 2.37 (s, 6H), 3.74 (m, 2H), 3.95 (m, 2H), 4.17 (m, 2H), 4.49 (m, 2H), 6.10 (d, 7.1 Hz, 2H), 6.84 (t, 7.9 Hz, 2H), 6.90 (d, 8.2 Hz, 4H), 7.00−7.07 (m, 12H), 7.36 (d, 8.2 Hz, 4H), 7.66−7.70 (m, 4H), 7.83−7.86 (m, 4H). ^{13}C-{^{1}H} NMR: (C_6D_6) δ 21.00 (s), 41.03 (s), 72.13 (d, 5.6 Hz), 73.28 (d, 5.3 Hz), 73.97 (d, 32.3 H), 74.97 (d, 8.8 Hz) 75.48 (d, 10.6 Hz), 79.34 (dd, 40.4 Hz, 6.3 Hz), 113.61 (d, 8.8 Hz), 122.17 (s), 123.18 (s), 127.72 (d, 9.3 Hz), 127.93 (d,9.3 Hz), 128.26 (s), 128.81 (s), 129.99 (d, 17.9 Hz), 133.33 (d, 50.3 Hz), 134.86 (d, 11.5), 135.41 (d, 13.3), 135.44 (d, 32.4 Hz), 136.62 (d, 2.8 Hz), 142.74 (dd, 124.3 Hz, 9.0 Hz), 147.41 (s), 153.45 (s). ^{31}P{^{1}H} NMR: (toluene) δ 14.1 (d, 33.4 Hz), 23.1 (d, 33.4 Hz). Anal. Calcd for $C_{56}H_{52}FeN_2P_2Pd$: C, 68.83; H, 5.36; N, 2.87. Found: C, 69.22; H, 5.48; N, 2.61.

Preparation of (DPPF)Pd(*p*-$CH_3OC_6H_4$)[N(*p*-$CH_3C_6H_4$)$_2$] (3c). Following the procedure for the preparation of **3a**, (DPPF)Pd(*p*-$CH_3OC_6H_4$)(I) (180 mg. 0.201 mmol) was reacted with KN(*p*-$CH_3C_6H_4$)$_2$ (52 mg, 0.221 mmol) in THF. Recrystallization at −35 °C from a concentrated THF solution layered with ether gave 143 mg of pure **3c** (74%). ^{1}H NMR: (C_6D_6) δ 2.23 (s, 6H), 3.17 (s, 3H), 3.72 (m, 2H), 3.95 (m, 2H), 4.15 (m, 2H), 4.50 (m, 2H), 6.26 (d, 8.1 Hz, 2H), 6.85 (d, 8.1 Hz, 2H), 6.90 (d, 8.2 Hz, 4H), 6.99−7.10 (m, 12H), 7.35 (d, 8.2 Hz, 4H), 7.62−7.69 (m, 4H), 7.80−7.86 (m, 4H). ^{13}C{^{1}H} NMR: (C_6D_6) δ 20.98 (s), 54.40 (s), 72.18 (d, 5.6 Hz), 73.35 (d, 5.2 Hz), 73.91 (d, 33.1 Hz), 74.94 (d, 9.2 Hz), 75.54 (d, 12.9 Hz), 79.08 (dd, 41.4 Hz, 7.0 Hz), 112.90 (d, 8.8 Hz), 122.13 (s), 123.38 (s), 127.72 (d, 9.4 Hz), 127.99 (d, 11.4 Hz), 128.24 (s), 128.83 (s), 130.12 (d, 3.8 Hz), 133.01 (d, 51.3 Hz), 134.75 (d, 12.5 Hz), 135.27 (d, 34.3 Hz), 135.36 (d, 12.5 Hz), 136.68 (d, 3.8 Hz), 146.68 (dd, 124.2 Hz, 9.6 Hz), 153.30 (s), 156.54 (s). ^{31}P{^{1}H} NMR: (toluene) δ 23.2 (d, 33.5 Hz), 14.6 (d, 33.5 Hz). Anal. Calcd for $C_{55}H_{49}FeNOP_2Pd$: C, 68.51; H, 5.12; N, 1.45. Found: C, 68.22; H, 4.98; N, 1.29.

Preparation of (DPPF)Pd(*p*-$CH_3C_6H_4$)[N(*p*-$CH_3C_6H_4$)$_2$] (3d). Following the procedure for the preparation of **3a**, (DPPF)Pd(*p*-$CH_3C_6H_4$)(I) (158 mg. 0.180 mmol) was reacted with KN(*p*-$CH_3C_6H_4$)$_2$ (52 mg, 0.221 mmol) in THF. Recrystallization at −35 °C from a concentrated THF solution layered with ether gave 116 mg of pure **3d** (68%). ^{1}H NMR: (C_6D_6) δ 1.94 (s, 3H), 2.23 (s, 6H), 3.73, (m, 2H), 3.95 (m, 2H), 4.16 (m, 2H), 4.48 (m, 2H), 6.40 (d, 6.3 Hz, 2H), 6.89−6.93 (m, 6H), 7.00−7.10 (m, 12H), 7.34 (d, 8.3 Hz, 4H), 7.62−7.66 (m, 4H), 7.81−7.85 (m, 4H); ^{31}P{^{1}H} NMR: (toluene) δ 23.6 (d, 34.2 Hz), 14.6 (d, 34.2 Hz). Anal. Calcd for $C_{55}H_{49}FeNP_2Pd$: C, 69.67; H, 5.21; N, 1.48. Found: C, 69.88; H, 5.42; N, 1.21.

Preparation of (DPPF)Pd(*p*-$CH_3SC_6H_4$)[N(*p*-$CH_3C_6H_4$)$_2$] (3e). Following the procedure for the preparation of **3a**, (DPPF)Pd(*p*-$CH_3SC_6H_4$)Br (210 mg. 0.241 mmol) was reacted with KN(*p*-$CH_3C_6H_4$)$_2$ (52 mg, 0.221 mmol) in THF. Recrystallization at −35 °C from a concentrated THF solution layered with ether gave 158 mg of pure **3e** (67%). ^{1}H NMR: (C_6D_6) δ 1.92 (s, 3H), 2.28 (s, 6H), 3.72 (m, 2H), 3.94 (m, 2H), 4.16 (m, 2H), 4.47 (m, 2H), 6.58 (d, 6.0 Hz, 2H), 6.83−7.10 (m, 18H), 7.31 (d, 8.2 Hz, 4H), 7.60−7.74 (m, 4H), 7.76−7.84 (m, 4H). ^{13}C{^{1}H} NMR: (C_6D_6) δ 20.96 (s), 21.37 (s), 72.29 (d, 5.4 Hz), 73.42 (d, 5.4 Hz), 73.78 (d, 35.7 Hz), 74.96 (d, 9.0 Hz), 75.55 (d, 13.0 Hz), 78.61 (dd, 41.6 Hz, 7.1 Hz), 122.16 (s), 123.56 (s), 125.63 (s), 126.43 (d 7.8 Hz), 127.82 (d 8.7 Hz), 128.34 (d, 11.6 Hz), 128.63 (s), 128.86 (s), 129.24 (s), 130.21 (s), 132.77 (d, 50.4 Hz), 134.62 (d, 11.0 Hz), 135.10 (d, 37.2 Hz), 136.88 (s), 153.19 (s), 156.02 (dd, 127.6 Hz, 7.3 Hz). ^{31}P{^{1}H} NMR: (toluene) δ 23.4 (d, 34.8 Hz), 14.6 (d, 34,8 Hz). Anal. Calcd for $C_{55}H_{49}FeNP_2PdS$: C, 67.39; H, 5.04; N, 1.43. Found: C, 67.02; H, 4.91; N, 1.74.

Preparation of (DPPF)Pd(*p*-ClC_6H_4)[N(*p*-$CH_3C_6H_4$)$_2$] (3f). Following the procedure for the preparation of **3a**, (DPPF)Pd(*p*-ClC_6H_4)-(I) (176 mg. 0.196 mmol) was reacted with KN(*p*-$CH_3C_6H_4$)$_2$ (51 mg, 0.217 mmol) in THF. Recrystallization at −35 °C from a concentrated THF solution layered with ether gave 118 mg of pure **3f** (62%). ^{1}H NMR: (C_6D_6) δ 2.22 (s, 6H), 3.70 (m, 2H) 3.94 (m, 2H), 4.13, (m, 2H), 4.45 (m, 2H), 6.57 (d, 6.7 Hz, 2H), 6.83−6.88 (m, 6H), 6.98−7.10 (m, 12H), 7.27 (d, 8.2 Hz, 4H), 7.55−7.62 (m, 4H), 7.75−7.82 (m, 4H). ^{13}C{^{1}H} NMR: (C_6D_6) δ 20.92 (s) 72.29 (d, 5.5 Hz), 73.42 (d, 7.9 Hz), 73.78 (d, 34.3 Hz), 74.91 (d, 8.6 Hz), 75.61 (d, 11.1 Hz), 78.38 (dd. 43.4 Hz, 8.2 Hz), 122.11 (s), 123.77 (s), 126.12 (d, 8,5 Hz), 127.73 (d, 8.5 Hz), 127.89 (s), 128.13 (d, 11.8 Hz), 128.25 (s), 128.88 (s), 130.29 (d, 11.8 Hz), 132.50 (d, 50.5 Hz), 134.51 (d, 11.4 Hz), 134.91 (d, 36.4 Hz), 135.31 (d, 12.8 Hz), 137.46 (s), 153.03 (s), 157.05 (dd, 125.2 Hz, 8.5 Hz). ^{31}P{^{1}H} NMR: (toluene) δ 23.5 (d, 34.2 Hz), 15.2 (d, 34.2 Hz); Anal. Calcd for $C_{54}H_{46}ClFeNP_2Pd$: C, 66.96; H, 4.79; N, 1.45. Found: C, 66.74; H, 4.95; N, 1.30.

Preparation of (PPh_3)Pd(C_6H_4-$C_6H_4NH_2$)(I) (4). Into a 50 mL screw-capped test tube, 602 mg (0.522 mmol) of Pd[P(C_6H_5)$_3$]$_4$ was

suspended in 25 mL of toluene. To this suspension, a solution of 231 mg (0.783 mmol) of 2′-amino-2-iodobiphenyl in 10 mL of toluene was added. The test tube was sealed and removed from the drybox. The reaction mixture was heated at 50 °C for 12 h during which time the product precipitated out of solution as a beige solid. The tube was taken back into the drybox, and the product was collected by filtration on a medium fritted funnel. The product was washed with 2 × 3 mL of Et_2O to yield 292 mg (84%) of **4**. ^{1}H NMR: ($CDCl_3$, 65 °C) δ 5.13 (broad, 2H), 6.51 (d, 4.0 Hz, 2H), 6.90 (m, 1H), 7.3−7.4 (m, 11H), 7.45−7.6 (m, 9H). ^{31}P NMR: (THF) δ 38.9. IR (cm^{-1}): (KBr) 3304 (m), 3233 (m), 3064 (w), 3034 (w), 1565 (m), 1492 (m), 1436 (m), 1100 (m), 1033 (s), 867 (m), 743 (s), 732 (s), 705 (s). Anal. Calcd for $C_{30}H_{25}NIPPd$: C, 54.28; H, 3.80; N, 2.11. Found: C, 54.22; H, 3.91; N, 2.14.

Preparation of *anti*-{[P(C$_6$H$_5$)$_3$]Pd(*p*-CH$_3$C$_6$H$_4$)(*μ*-NH-*t*-Bu)}$_2$ (6). Into a 20 mL vial was weighed 352 mg (0.415 mmol) of $[P(C_6H_5)_3]_2$-Pd(*p*-$CH_3C_6H_4$)(I). This material was suspended in 10 mL of Et_2O and to the resulting suspension was added 36 mg (0.46 mmol) of LiNH-*t*-Bu as a solid. The reaction was stirred for 24 h, over which time the white suspension became pale yellow. The Et_2O was decanted from the solid. Fresh Et_2O (10 mL) was then added and 15 mg (0.069 mmol) of *p*-$CH_3C_6H_4I$ was added to react with the $Pd(PPh_3)_4$ byproduct. After 15 min, the solid was isolated by filtration using a medium fritted funnel. The solid was then extracted with 3 × 4 mL of toluene, leaving behind the palladium halide complex. The toluene was then concentrated. The product began to crystallize upon concentration and was isolated by pipetting off the supernatant. Pentane (10 mL) was then added to the supernatant to isolate the remaining product. The solvent mixture was cooled at −35 °C for 5 h. The total yield was 46 mg (20%). ^{1}H NMR: (C_6D_6) δ −0.10 (d, 5.3 Hz, 2H), 1.27 (s, 18H), 2.20 (s, 6H), 6.65 (broad s, 2H), 6.90 (broad s, 2H) 6.95−7.06 (m, 18H), 7.55 (broad s, 2H), 7.59 (broad s, 2H), 7.61(t, 8.4 Hz, 12H). ^{1}H NMR: (C_6D_6, 75 °C) δ −0.07 (d, 5.3 Hz, 2H), 1.26 (s, 18H), 2.16 (s, 6H), 6.71 (d, 6.0 Hz, 4H), 6.91-7.09 (m, 18H), 7.26 (d, 6.0 Hz, 4H), 7.5(t, 8.4 Hz, 12H). ^{31}P NMR: (toluene) δ 25.7. IR (cm^{-1}): (KBr) 3301 (w), 3070 (w), 3050 (m), 2957 (m), 2916 (m), 2861 (m), 1582 (m), 1481 (s), 1432 (s), 1384 (m), 1358 (m), 1350 (m), 1187 (s), 1096 (s), 1010 (s), 917 (s), 905 (s) 791 (s), 746 (s), 698 (s). Anal. Calcd for $C_{58}H_{64}N_2P_2Pd_2$: C, 65.48; H, 6.06; N, 2.63. Found: C, 65.49; H, 6.09; N, 2.55.

Preparation of *anti*-{[P(C$_6$H$_5$)$_3$]Pd(C$_6$H$_5$)(*μ*-NHC$_6$H$_5$)}$_2$ (7). In a 20 mL vial, 283 mg (0.339 mmol) of $(PPh_3)_2Pd(Ph)I$ was stirred in 15 mL of toluene. To this suspension was added 66.8 mg (0.509 mmol) of KNHPh as a solid. The reaction was stirred at room temperature for 2 h. A ^{31}P{^{1}H} NMR spectrum of the reaction mixture indicated complete consumption of $(PPh_3)_2Pd(Ph)I$ and the formation of **7** and $Pd(PPh_3)_4$. The reaction mixture was filtered through Celite, and the toluene solvent was removed by vacuum to obtain a dry solid. To the resulting solids was added 6 mL of fresh toluene. This suspension was stirred for 2 h to extract $Pd(PPh_3)_4$ from the product **7**. The suspension was filtered through a medium fritted funnel, and **7** was collected as a solid. Recrystallization of the solid at −35 °C from a concentrated THF solution layered with Et_2O gave pure crystalline **7** in 28% yield (50.2 mg). ^{1}H NMR: (toluene-d_8) δ 1.22 (d, 4.3 Hz, 1H), 1.42 (d, 5.3 Hz, 1H), 6.58−6.69 (m, 4H), 6.74−6.99 (m, 16H), 7.11−7.16 (m, 18H), 7.24−7.44 (m, 12H); ^{31}P NMR (THF) δ 29.73 (s), 29.69 (s). IR (cm^{-1}): (KBr) 3307 (w), 3044 (m), 3028 (m), 2998 (w), 2966 (w), 2922 (w), 1592 (s), 1564 (s), 1485 (s), 1471 (m), 1437 (s), 1340 (w), 1310 (w), 1226 (s), 1205 (m), 1100 (s), 1063 (m), 1023 (s), 998 (m), 816 (s), 742 (s). Anal. Calcd for $C_{60}H_{52}N_2P_2Pd_2$: C, 66.99; H, 4.87; N, 2.60. Found: C, 66.81; H, 4.79; N, 2.54.

Generation of [(PPh$_3$)Pd(C$_6$H$_4$-C$_6$H$_4$NH)]$_2$ (5). A solution of 10 mg (0.015 mmol) of $(PPh_3)Pd(C_6H_4\text{-}C_6H_4NH_2)(I)$ in 0.5 mL of toluene-d_8 was placed in an NMR tube and cooled at −40 °C. To the cooled solution was added a solution of 3.0 mg (0.015 mmol) of $KN(TMS)_2$ in 0.2 mL of toluene-d_8. The tube was placed into an NMR probe which had been cooled to −40 °C. The NMR probe was slowly heated until reaction occurred at −15 °C. ^{1}H NMR: (toluene-d_8, 20 °C) δ 1.96 (d, 7.6 Hz, 1H), 6.54 (t, 7.2 Hz, 1H), 6.62 (m, 1H), 6.73 (t, 7.4 Hz, 1H), 6.80−6.97 (m, 12H), 7.43−7.50 (m, 8H). ^{31}P NMR: (THF) δ 31.9. IR (cm^{-1}) (C_7D_8): 3289 (w, NH).

Generation of (DPPF)Pd(Ph)(NH-*i*-Bu) (8a). (DPPF)Pd(Ph)(I) (12.1 mg, 0.0140 mmol) was suspended in 0.6 mL of toluene, and the solution was transferred to an NMR tube. The NMR tube was cooled at −35 °C in the drybox freezer. LiNH-*i*-Bu (1.6 mg, 0.020 mmol) was added to the NMR tube as a solid. The tube was quickly placed in the NMR: probe at −80 °C. The probe was warmed until reaction occurred at 0 °C. ^{31}P{^{1}H} NMR: (toluene, 0 °C) δ 26.5 (d, 22.0 Hz), 18.3 (d, 22.0 Hz). Selected resolved ^{1}H NMR resonances: (C_7D_8) δ 2.55 (m, CH_2), 1.96 (m, NH), 0.53, d, 7.5 Hz, CH_3).

Generation of (DPPF)Pd(Ph)(NHPh) (8b). (DPPF)Pd(Ph)(I) (12.6 mg, 0.0146 mmol) was suspended in 0.6 mL of THF, and the solution was transferred to an NMR tube. The NMR tube was cooled at −35 °C in the drybox freezer. KNHPh (2.1 mg, 0.016 mmol) was added to the NMR tube as a solid. The tube was quickly placed in the NMR probe cooled at −80 °C. The probe was incrementally warmed until reaction occurred at 0 °C. ^{31}P{^{1}H} NMR: (THF, 0 °C) δ 25.1 (d, 38 Hz), 6.3 (d, 38 Hz).

Generation of 8b with [^{15}N]KNHPh. (DPPF)Pd(Ph)(I) (15.0 mg, 0.0174 mmol) was dissolved in 0.4 mL of THF. [^{15}N]KNHPh (2.4 mg, 0.018 mmol) was dissolved in 0.2 mL of THF, and the two solutions were combined. The reaction mixture was transferred to an NMR tube and quickly placed in the NMR probe cooled to 0 °C. ^{31}P-{^{1}H} NMR: (THF, 0 °C) δ 25.1 (dd, J_{PP} = 38 Hz, J_{NP} = 43 Hz) 6.3 (dd, J_{PP} = 38 Hz, J_{NP} = 4 Hz). ^{15}N{^{1}H} NMR: (THF, 0 °C) δ 69.5 (d, J_{NP} = 43 Hz).

Generation of 9 with [^{15}N]KNHPh. (DPPF)Pd(Ph)(I) (15.4 mg, 0.0178 mmol) was dissolved in 0.6 mL of THF. [^{15}N]KNHPh (22.1 mg, 0.167 mmol) was added as a solid. The reaction was transferred to an NMR tube and quickly placed into the NMR probe, which was cooled to 0 °C. ^{31}P{^{1}H} NMR: (THF, 0 °C) δ 22.3 (d, J_{NP} = 46 Hz), −16.6 (s); ^{15}N{^{1}H} NMR: (THF, 0 °C) δ 89.2 (s), 86.5 (d, J_{NP} = 46 Hz).

Preparation of *anti*-{[P(C$_6$H$_5$)$_3$]Pd(C$_6$H$_5$)(*μ*-NH-*t*-Bu)}$_2$ (6b). Into a 20 mL vial was weighed 357 mg of $[P(C_6H_5)_3]_2Pd(C_6H_5)(I)$ (0.428 mmol). This material was suspended in 15 mL of Et_2O, and 27 mg (.34 mmol) of LiNH-*t*-Bu was added to the suspension as a solid. The reaction mixture was stirred for 2 h. To the reaction mixture was then added 30 mg (0.147 mmol) of C_6H_5I, and the resulting solution was stirred for an additional 30 min. The reaction was filtered through a medium fritted funnel to remove the solid palladium aryl halide complex. The ether was removed under vacuum to give a yellow oily residue. The oily residue was layered with pentane and cooled at −35 °C for 12 h to give 62 mg (28%) of product. ^{1}H NMR: (C_6D_6, 55 °C) δ −0.11 (d, 4.8 Hz, 2H), 1.22 (s, 18H), 6.86 (t, 5.3 Hz, 4H), 6.90−7.13 (m, 24H), 7.26 (t, 8.2 Hz, 12H). ^{31}P NMR: (toluene) δ 26.0. IR (cm^{-1}): (KBr) 3317 (w), 3303 (w), 3049 (s), 2955 (s), 2861 (m), 1563 (s), 1479 (m), 1468 (m), 1434 (s), 1354 (w), 1185 (s), 1094 (s) 1058 (w), 1021 (m), 996 (w), 922 (w), 906 (w), 888 (w), 804 (w) 745 (m), 729 (s), 697 (s).

Kinetic Analysis of the Reductive Elimination Reaction of 1. Into a vial was weighed 20 mg (0.023 mmol) of **1**. The solid was dissolved in approximately 5 mL of anhydrous THF and transferred to a 10 mL volumetric flask. The volumetric flask was then filled with enough THF to make 10 mL of a 0.0023 M solution. Into another vial was weighed the appropriate amount of PPh_3. A 4.5 mL aliquot of the palladium solution was syringed from the volumetric flask into the vial containing the phosphine. Once all of the phosphine was dissolved, the solution was transferred into a quartz UV−vis cell equipped with a stopcock. The reaction was heated at 80 °C in a constant temperature water bath and a UV−vis spectrum was taken every 30 min. The concentration of palladium amide was monitored at λ = 489.6 nm throughout the course of the reaction. The following pseudo-first-order rate constants were obtained at different concentrations of PPh_3 (k, [PPh_3]): 1.7 × 10^{-4} s^{-1}, 0.023 M; 1.3 × 10^{-4} s^{-1}, 0.034 M; 8.0 × 10^{-5} s^{-1}, 0.045 M; 7.3 × 10^{-5} s^{-1}, 0.057 M; 4.8 × 10^{-5} s^{-1}, 0.068 M.

Kinetic Analysis of the Reductive Elimination Reaction of 2. Into a vial was weighed 30.2 mg (0.0334 mmol) of **2**. The solid was dissolved in approximately 3 mL of toluene-d_8 and transferred into a 5 mL volumetric flask. The volumetric flask was filled with toluene-d_8 to make 5 mL of a solution that had [**2**] = 0.0067 M. Triphenylphosphine-d_{15} was weighed into a separate vial. A 0.5 mL aliquot of the volumetric solution was transferred by syringe to the vial containing the phosphine. Upon dissolution of the phosphine, the solution was transferred to an NMR tube. The tube was cooled in a dry ice/acetone bath and flame sealed. This procedure results in a tube

sealed at atmospheric pressure at room temperature. Reaction rates were measured by ^{1}H NMR spectroscopy at 110 °C. Samples were shimmed at room temperature and removed. The NMR probe was then heated to 110 °C. The sample was placed into the probe, quickly reshimmed, and an automated program was initiated that collected single pulse experiments with at least 1 min between data acquisitions. The resonance for the tolyl CH_3 was used to monitor the concentration of palladium amido complex throughout the course of the reaction. The following pseudo-first-order rate constants were obtained at different concentrations of PPh_3 (k, [PPh_3]): 5.0×10^{-3} s^{-1}, 0.052 M; 4.0×10^{-3} s^{-1}, 0.061 M; 4.4×10^{-3} s^{-1}, 0.079 M; 3.3×10^{-3} s^{-1}, 0.087 M; 3.2×10^{-3} s^{-1}, 0.10 M; 2.6×10^{-3} s^{-1}, 0.14 M; 2.4×10^{-3} s^{-1}, 0.16 M; 2.2×10^{-3} s^{-1}, 0.19 M; 2.0×10^{-3} s^{-1}, 0.19 M; 1.2×10^{-3} s^{-1}, 0.47 M.

Kinetic Analysis of the Reductive Elimination Reaction of 3a−f. A stock solution was made by dissolving 101 mg (0.385 mmol) of PPh_3 in 3.5 mL of toluene-d_8. The palladium amido complex was weighed into a small vial: 5.9 mg (0.0063 mmol) **3a**, 6.2 mg (0.0064 mmol) **3b**, 6.1 mg (0.0063 mmol) **3c**, 6.0 mg (0.0063 mmol) **3d**, 6.2 mg (0.0063 mmol) **3e**, 6.1 mg (0.0063 mmol) **3f**. A 0.5 mL aliquot of the PPh_3 stock solution was transferred by syringe into each of the six vials. Upon dissolution, each sample was transferred to an NMR sample tube. The tubes were frozen in N_2(l) and flame sealed, resulting in a tube sealed at atmospheric pressure at room temperature. Reaction rates were measured by ^{1}H NMR spectroscopy at 75 °C using a procedure analogous to that for monitoring reaction of **2**. The results of the kinetic analysis are summarized in Table 2.

Phosphine Dependence on the Reductive Elimination Reaction of 3f. A stock solution was prepared by dissolving 12.1 mg (0.0126 mmol) of **3f** in 1.2 mL of toluene-d_8. PPh_3 (6.9 mg, 0.026 mmol or 20.6 mg, 0.079 mmol) was weighed into a small vial. A 0.5 mL aliquot of the stock solution was transferred to each of the two vials. Upon dissolution, each sample was transferred to an NMR tube. The tubes were frozen in N_2(l) and flame sealed, resulting in a tube sealed at atmospheric pressure at room temperature. Reaction rates were measured by ^{1}H NMR spectroscopy at 75 °C as described above.

Kinetic Analysis of the Reductive Elimination Reaction of 6. Triphenylphosphine (6.8 mg, 0.026 mmol or 20.2 mmol 0.0771 mmol) and **6** (3.0 mg, 0.0043 mmol or 7.2 mg, 0.010 mmol) and a small amount (<1 mg) of trimethoxybenzene were weighed into the same vial. Toluene-d_8 (0.65 mL) was syringed into each vial to dissolve the solids. Once the solids were dissolved, the solutions were transferred to NMR tubes. The tubes were frozen in N_2(l) to create a vacuum and were flame sealed. This procedure results in a tube sealed at atmospheric pressure. The samples were heated at 95 °C in a constant temperature water bath, and ^{1}H NMR spectra were taken periodically. The concentration of palladium amide complex was measured by the integration of the NH resonance or tolyl resonance relative to the trimethoxybenzene internal standard. The results of the kinetic analysis are summarized in Table 3.

Kinetic Analysis of the Reductive Elimination Reaction of 7. A stock solution was prepared by dissolving 30 mg of triphenylphosphine-d_{15} (0.11 mmol) in 1.2 mL of toluene-d_8. Compound **7** (3.1 mg, 0.0029 mmol or 12.1 mg, 0.0113 mmol) was weighed into a small vial with a small amount (<1 mg) of trimethoxybenzene. A 0.5 mL aliquot of the stock solution was transferred by syringe to each of the vials to dissolve the solids. The solutions were transferred to NMR tubes. The tubes were frozen in N_2(l) to create a vacuum and were flame sealed. This procedure results in a tube sealed at atmospheric pressure. The samples were heated at 95 °C in a constant temperature water bath, and ^{1}H NMR spectra were taken periodically. The concentration of palladium amide complex was measured by the integration of an aromatic or NH resonance relative to the trimethoxybenzene internal standard. The results of the kinetic analysis are summarized in Table 3.

Phosphine Dependence of the Reductive Elimination Reaction of 7. Triphenylphosphine-d_{15} (5.3 mg, 0.019 mmol or 15.9 mg, 0.0573 mmol) and **7** (4.1 mg, 0.0038 mmol) were weighed into the same small vial along with a small amount (<1 mg) of trimethoxybenzene. Toluene-d_8 (0.4 mL) was syringed into the vials to dissolve the solids. The solutions were transferred to NMR tubes and sealed as described above. Kinetic data was obtained as described above. The results of the kinetic analysis are summarized in Table 3.

X-ray Structure of 3b. A red plate crystal of $C_{56}H_{52}N_2P_2FePd\cdot C_3H_6O_{0.75}$ having approximate dimensions of 0.08 × 0.10 × 0.24 mm was obtained by layering a THF solution of **3b** with ether at −35 °C and was mounted on a glass fiber. Data was collected at −60 °C on an Enraf-Nonius CAD-4 diffractometer with graphite monochromated Mo Kα radiation.

Cell constants and an orientation matrix for data collection obtained from a least-squares refinement using the setting angles of 18 carefully centered reflections in the range $5.24 < 2\theta < 13.47°$ corresponded to a triclinic cell with dimensions given in Table 2. On the basis of packing considerations, a statistical analysis of intensity distribution, and the successful solution and refinement of the structure the space group was determined to be: P_{-1} (no. 2).

Of the 10 832 reflections which were collected 10 281 were unique ($R_{int} = 0.109$). The intensities of three representative reflections, which were measured after every 60 min of X-ray exposure time, remained constant throughout data collection indicating crystal and electronic stability (no decay correction was applied). The linear absorption coefficient for Mo Kα is 7.4 cm^{-1}. Azimuthal scans of several reflections indicated no need for an absorption correction. The data were corrected for Lorentz and polarization effects.

The structure was solved by the Patterson method. The non-hydrogen atoms were refined anisotropically. The hydrogen atoms were included in calculated positions. In the case of the methyl group hydrogens, one hydrogen atom was located in the difference map and included at an idealized distance to set the orientation of the other hydrogen atoms. The THF solvent molecule appeared disordered and the multiplicity of the THF molecule was approximately 0.75%.

The standard deviation of an observation of unit weight was 1.49. The weighting scheme was based on counting statistics and included a factor ($p = 0.02$) to downweight the intense reflections. Plots of $\sum w(|F_o| - |F_c|)^2$ versus $|F_o|$, reflection order in data collection, sin θ/λ, and various classes of indices showed no unusual trends. The maximum and minimum peaks on the final difference Fourier map corresponded to 0.67 and −0.51 e/Å^3 respectively.

Neutral atom scattering factors were taken from Cromer and Waber.[99] Anomalous dispersion effects were included in F_{calc}; the values for $\Delta f'$ and $\Delta f''$ were those of Cromer. All calculations were performed using the TEXSAN crystallographic software package of Molecular Structure Corporation.

Acknowledgment. This work was generously supported by the Department of Energy (DE-RG02-96ER14678). We also gratefully acknowledge support from a DuPont Young Professor Award, a Union Carbide Innovative Recognition Award, a National Science Foundation Young Investigator Award, and a Dreyfus Foundation New Faculty Award, and a Camille Dreyfus Teacher−Scholar award for support for this work. J.F.H. is a fellow of the Alfred P. Sloan Foundation. We thank Johnson-Matthey Alpha/Aesar for donation of palladium chloride.

Supporting Information Available: Tables of positional parameters and B(eq), U values, intramolecular distances, intramolecular bond angles, Cartesian coordinates, and torsion or conformational angles for hydrogen and non-hydrogen atoms and a fully labeled PLUTO diagram (21 pages). See any current masthead page for ordering and Internet access instructions. (**3b**).

JA971057X

(99) Cromer, D. T.; Waber, J. T. *International Tables for X-ray Crystallography*; The Kynoch Press: Birmingham England, 1974; Vol. IV, Table 2.3.1.